Politecnico di Torino

Master's Degree

in

Energy and Nuclear Engineering

Modeling and Analysis of Thermal Runaway in a Lithium-Ion Cell

Supervisor

Davide Papurello

Candidate

Samuele Salerno

Academic Year 2024 - 2025

CONTENTS

Abstract **5**

1 Introduction **6**

1.1 Background and Motivation 6

1.2 Thermal Runaway Phenomenon 10

1.3 Objectives of the Thesis 11

2. Thermal Runaway in Lithium-Ion Batteries **13**

2.1 Definition of Thermal Runaway 13

2.2 Triggering Mechanisms 14

2.2.1 Electrical Abuse 15

2.2.2 Thermal Abuse 17

2.2.3 Mechanical Abuse 18

2.3 Exothermic Reactions and Runaway Sequence 20

2.4 Effects and Consequences on the Cell 22

3. Physical Modeling of the Battery **25**

3.1 State of Art of Thermal Runaway Model 25

3.2 Modeling Approach 27

3.3 Electrochemical Model 28

3.3.1 Porous Electrode Theory 28

3.3.2 Electrochemical Equation 30

3.4 Thermal Model 42

3.4.1 Arrhenius Heat 47

3.5 Electrochemical–Thermal Coupling 52

3.6 Model Assumptions and Limitations 55

4. Implementation of the Model in COMSOL Multiphysics **56**

4.1 Description of the COMSOL Environment 56

4.1.1 Mesh in Comsol 58

4.2 Physics and Mathematics Implemented 60

4.2.1 Electrochemical Model in Comsol 60

4.2.2 Thermal Model in Comsol 65

4.3 Coupled Physics Setup 66

4.4 Initial Conditions 70
4.5 Implementation of Thermal Runaway Mechanisms 71
4.6 Numerical Solution Strategy 73
5. Experimental Campaign 75
5.1 Objectives of the Experimental Tests 75
5.2 Description of the Tested Cells 76
5.3 Instrumentation and Data Acquisition 77
5.4 Experimental Results 79
6. Results and Model Validation 83
6.1 Model Results 83
6.2 Model–Experiment Comparison 92
6.2.1 Analysis of Absolute Temperature Profiles 92
6.2.2 Normalized Data Analysis and Temporal Dynamics 93
6.3 Discussion of Results 95
6.4 Model Accuracy and Limitations 95
7. Conclusions and Future Developments 96
Nomenclature 101
References 102

Abstract

Lithium-ion batteries are increasingly used in modern society, enabling the widespread adoption of portable electronics, electric vehicles, and renewable energy storage systems. Their high energy density and long cycle life have made them the dominant energy storage technology across multiple sectors. However, safety remains a critical challenge, particularly under abusive operating conditions that may lead to thermal runaway, a rapid and self-accelerating increase in temperature that can result in fire or explosion.

Understanding the mechanisms governing thermal runaway is essential for improving battery reliability and developing effective mitigation strategies. In this work, a numerical model of a lithium-ion cell is developed to investigate conditions leading to thermal instability after mechanical abuse and to analyze the dynamic interaction between electrochemical processes and heat generation.

The study focuses on the coupled nature of electrochemical reactions, internal heat production, and temperature evolution within the cell. The model is employed to explore scenarios in which abnormal conditions, such as increased internal resistance or the presence of an internal short circuit, may trigger uncontrolled temperature growth.

Through a systematic numerical investigation, the work identifies critical factors influencing the onset of thermal runaway and examines the relative contribution of different heat sources during the transition from stable operation to runaway conditions. The results highlight the importance of nonlinear thermal–electrochemical coupling in determining cell stability and help to better understand the mechanisms that govern the escalation process.

The numerical results are compared with experimental data obtained from dedicated tests carried out within the scope of this work to assess the predictive capability of the model and to evaluate its ability to reproduce the main features of thermal runaway behavior. This comparison allows for a critical validation of the modeling approach and supports the physical consistency of the adopted framework.

Overall, this work contributes to a better understanding of the mechanisms governing thermal instability at the cell level and supports the development of safer and more reliable lithium-ion battery systems.

1 Introduction

1.1 Background and Motivation

In recent decades, the European energy system has undergone a profound transformation, driven by the need to ensure security of supply, economic competitiveness, and, above all, environmental sustainability. The European Union, historically highly dependent on fossil fuel imports, is now facing a dual challenge: on the one hand, reducing greenhouse gas emissions responsible for climate change; on the other, transitioning towards an energy model based on renewable sources, energy efficiency, and electrification of final consumption.

Greenhouse gas emissions primarily carbon dioxide (CO_2), methane (CH_4), and nitrous oxide (N_2O) are closely linked to the energy sector, which includes electricity generation, transportation, industry, and residential heating. Although Europe has achieved a progressive reduction in emissions over the past decades, the energy sector remains the largest contributor to climate-altering emissions. The growing

scientific evidence of global warming effects such as rising average temperatures, increasing frequency of extreme weather events, melting ice caps, and sea level rise has made coordinated international action essential.

Within this global framework, international climate agreements have played a crucial role. The Paris Agreement[1] established a legally binding framework aimed at limiting the global temperature increase to well below 2°C above pre-industrial levels, while pursuing efforts to restrict it to 1.5°C. Subsequent Conferences of the Parties (COP)[2] under the United Nations Framework Convention on Climate Change have focused on strengthening national commitments and implementation mechanisms. In particular, COP25, held in Madrid in 2019 under the Chilean presidency, emphasized the urgency of increasing ambition in emission reduction targets and accelerating global climate action.

At the European level, the European Union has positioned itself as a global leader in climate policy. A central pillar of this strategy is the European Green Deal[3], presented in 2019, which sets out a comprehensive roadmap to make Europe the first climate-neutral continent by 2050. The Green Deal is not merely an environmental initiative; it represents a broad economic and industrial transformation strategy encompassing energy, mobility, construction, agriculture, and manufacturing sectors. As an intermediate milestone, the EU has committed to reducing net greenhouse gas emissions by at least 55% by 2030 compared to 1990 levels, a target formalized through the Fit for 55 legislative package.

Outside Europe, the energy transition follows heterogeneous pathways, strongly shaped by domestic political dynamics, economic priorities, and the availability of natural resources. In the United States, the decarbonization trajectory has been marked by significant political discontinuity. After rejoining the Paris Agreement in 2021, the subsequent administration led by Donald Trump initiated a new withdrawal from the agreement, signaling a renewed emphasis on expanding domestic oil and gas production. This alternating policy direction reflects the ongoing tension between climate objectives, energy security, and industrial competitiveness that characterizes the U.S. energy debate.

China, by contrast, has adopted a more structured and long-term strategy. While remaining the world's largest CO_2 emitter and continuing to rely significantly on coal to sustain economic growth and power system stability, China is also the leading global investor in renewable energy and a dominant manufacturer of photovoltaic modules, wind turbines, and lithium-ion batteries. Its energy transition can therefore be described as gradual and strategic, aiming to balance energy security, industrial development, and a progressive reduction in carbon intensity.

Australia presents a distinctive case. Although its economy is heavily linked to the extraction and export of coal and natural gas, the country is rapidly increasing the share of electricity generated from renewable sources, particularly solar and wind, thanks to its abundant natural resources. However, the economic relevance of the fossil fuel sector makes the Australian transition complex, requiring a continuous balance between climate commitments and economic interests.

Overall, the extra-European landscape highlights that the energy transition is a global yet uneven process, deeply influenced by national

political priorities and by each country's strategic position within the international energy system.

The European energy transition is structured around three main pillars: increasing the share of renewable energy sources, improving energy efficiency, and promoting the electrification of end-use sectors, particularly transportation. In recent years, electric mobility has experienced rapid growth, driven by technological progress, stricter emission regulations, and supportive public policies. The widespread diffusion of electric vehicles (EVs) offers several environmental advantages, most notably the reduction of local pollutant emissions and the potential decrease in greenhouse gas emissions when electricity is generated from low-carbon sources. Furthermore, electric drivetrains typically exhibit higher energy efficiency compared to internal combustion engines. However, the large-scale adoption of electric mobility also presents challenges, including the need for extensive charging infrastructure, concerns related to battery production and raw material supply chains, and the impact of increased electricity demand on power grids.

In parallel, the growing penetration of renewable energy sources such as solar and wind introduces additional complexity to power system management due to their intrinsic variability and intermittency. Unlike conventional fossil-fuel-based power plants, renewable generation is strongly dependent on weather conditions and therefore does not always match electricity demand. In this context, energy storage systems play a crucial role in ensuring grid stability and reliability. Storage technologies

allow excess electricity generated during periods of high renewable production to be stored and later released when generation is low or demand is high, thereby smoothing fluctuations in power supply. Among the various available technologies, electrochemical storage, particularly lithium-ion batteries, has emerged as a key solution due to its high efficiency, scalability, and rapid response time.

Consequently, the development and optimization of battery technologies are fundamental for enabling both the widespread deployment of renewable energy and the continued expansion of electric mobility within a sustainable energy system.

Within this regulatory, environmental, and technological framework, scientific research and innovation are essential to support the transition towards a sustainable and low-carbon energy system. This thesis is situated within this broader context, contributing to the study and development of technological solutions aligned with European decarbonization objectives and global climate mitigation efforts.

1.2 Thermal Runaway Phenomenon

A crucial aspect in the development and widespread adoption of batteries, particularly lithium-ion batteries, is thermal safety. During operation, batteries generate heat due to several mechanisms, including ohmic losses, electrochemical reactions, and mass transport processes occurring within the cell. Under normal operating conditions, this heat can be effectively managed through appropriate thermal management systems. However, under abnormal conditions such as overcharging, internal or external short circuits, mechanical damage, or high ambient temperatures

heat generation can increase significantly, potentially leading to a phenomenon known as Thermal Runaway.

Thermal runaway is a self-accelerating process in which exothermic reactions inside the cell cause a rapid rise in temperature and internal pressure. This process can trigger the decomposition of electrolyte and electrode materials, potentially leading to the release of flammable gases and, in severe cases, fires or explosions. For this reason, thermal safety represents a key factor not only for ensuring the reliability and lifetime of battery systems, but also for enabling their safe use in large-scale applications such as electric vehicles and grid-level energy storage systems.

For these reasons, a thorough understanding of the thermal phenomena occurring inside batteries is essential for the development of predictive models, effective thermal management strategies, and improved design solutions aimed at preventing hazardous operating conditions. In this context, numerical modeling and simulation of electrochemical and thermal processes represent fundamental tools for analyzing battery behavior under different operating conditions and for supporting the development of safer and more reliable energy storage technologies.

1.3 Objectives of the Thesis

The main objective of this thesis is the development and validation of a numerical model capable of realistically describing the thermal behavior of a battery under critical operating conditions. In particular, the work

focuses on the comparison between simulation results and experimental data, with the aim of verifying the model's ability to reproduce the physical phenomena observed in real systems.

Through this process of comparison and validation, the goal is to obtain a reliable simulation tool capable of accurately representing the evolution of thermal variables within the cell under different operating conditions. A properly calibrated model not only allows the interpretation of experimentally observed phenomena but also makes it possible to investigate operating scenarios that are difficult or dangerous to study through direct experimentation, thereby reducing time, costs, and risks associated with experimental testing.

In this context, numerical modeling represents a powerful tool to support the design and optimization of electrochemical energy storage systems. The ability to predict the thermal behavior of batteries makes it possible to identify potentially hazardous operating conditions and to develop strategies and design solutions aimed at improving the safety of battery-based systems, ultimately contributing to the development of safer and more reliable energy storage technologies.

During the experimental tests, several cells with different capacities were used, and the model was designed to adapt to different specifications. However, the results presented in this work refer to a Samsung INR18650-35E (Version 3) with a capacity of 3400 mAh, a lithium-ion cell that employs a graphite negative electrode and an NMC (Lithium Nickel Manganese Cobalt Oxide) positive electrode [4]

2. Thermal Runaway in Lithium-Ion Batteries

2.1 Definition of Thermal Runaway

The phenomenon of Thermal Runaway represents one of the main safety concerns associated with lithium-ion batteries. It consists of a rapid and uncontrolled increase in temperature caused by a series of exothermic reactions occurring inside the cell. Thermal runaway occurs when the heat generated within the battery exceeds the system's ability to dissipate it to the surroundings. Under these conditions, the temperature rise accelerates further heat generation, creating a positive feedback mechanism that can ultimately lead to severe cell degradation, gas release, fire, or even explosion. Moreover, thermal runaway is an irreversible process: once initiated, the rate of heat generation becomes greater than the heat that can be removed from the system, making it impossible to restore thermal equilibrium. As a result, the process self-sustains and progresses uncontrollably, driving the cell toward increasingly higher temperatures and irreversible damage.

From a technical point of view, thermal runaway does not occur instantaneously but develops through several stages as the temperature increases, each associated with specific physical and chemical processes.

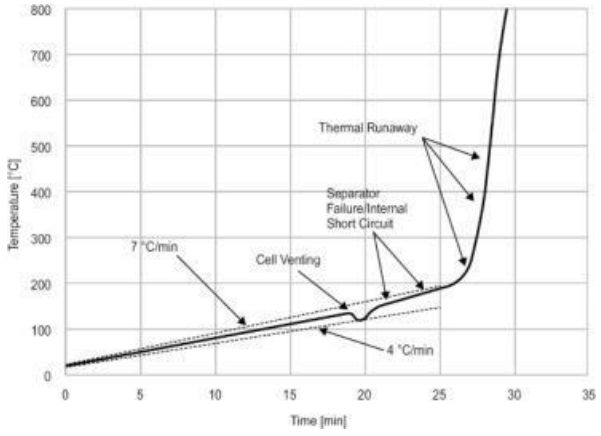

Figure 1 Phase of thermal runaway [5]

2.2 Triggering Mechanisms

The onset of Thermal Runaway in lithium-ion batteries can be initiated by different types of abuse conditions that destabilize the internal electrochemical and thermal equilibrium of the cell. In general, the main triggering mechanisms are commonly classified into three categories[5]: thermal abuse, electrical abuse, and mechanical abuse. Although these mechanisms originate from different external causes, they often lead to similar internal effects, such as excessive heat generation, internal short circuits, or accelerated degradation of cell components

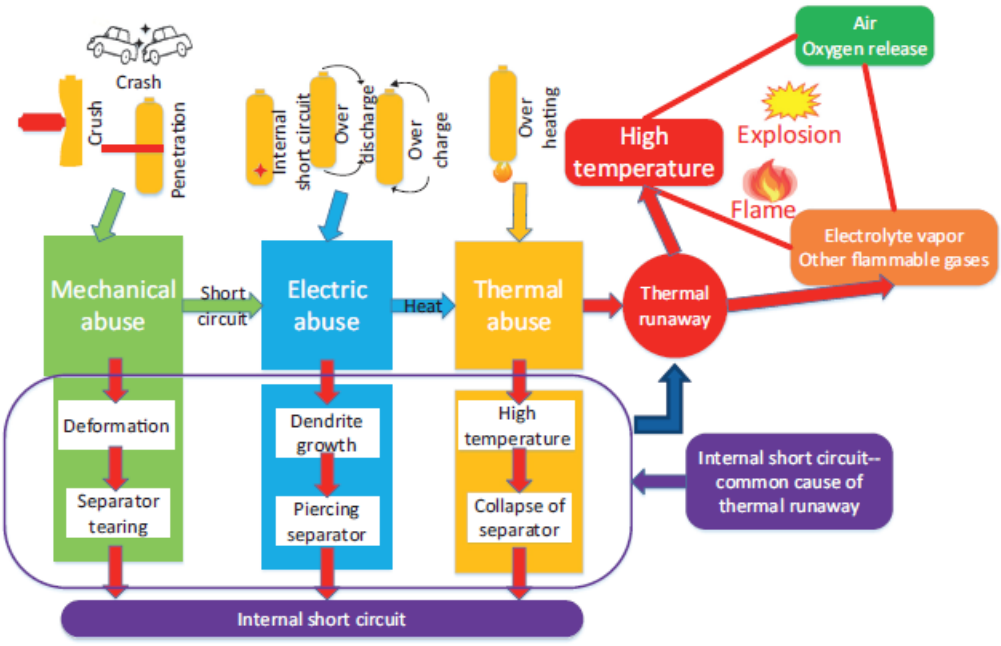

Figure 2 Triggering mechanism [5]

2.2.1 Electrical Abuse

Electrical abuse occurs when the cell operates outside its safe electrical limits. This type of abuse typically includes conditions such as overcharging, overdischarging, and external short circuits. These situations can significantly disturb the electrochemical balance of the battery, leading to excessive heat generation, structural degradation of the electrodes, and potentially the initiation of internal short circuits.

One of the most critical forms of electrical abuse is overcharging, which takes place when the battery continues to receive current after reaching its maximum allowable voltage. Under these conditions, the normal intercalation process of lithium ions into the negative electrode becomes unstable. As the anode becomes fully saturated with lithium, additional lithium ions may start to deposit on the surface of the graphite electrode in the form of metallic lithium plating rather than being intercalated into the electrode structure. This metallic lithium can form dendritic structures that grow through the separator, potentially causing internal short circuits between the anode and cathode.

At the same time, overcharging can destabilize the cathode material. When the cell voltage exceeds its designed limits, the positive electrode may undergo structural degradation and decomposition reactions that release heat and, in some cases, oxygen. These reactions are highly exothermic and contribute to the overall thermal instability of the cell.

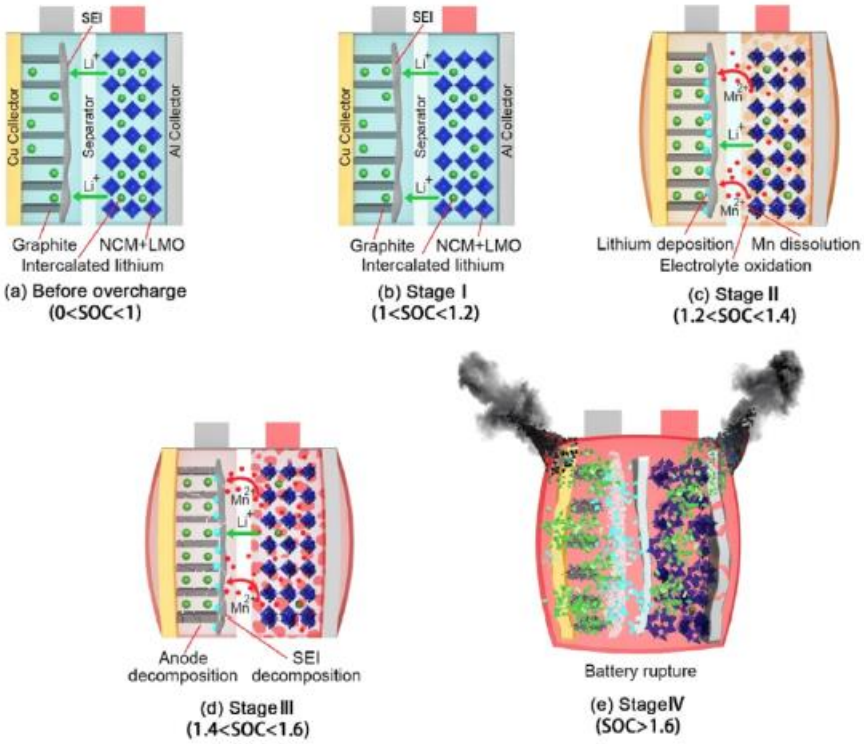

Figure 3 overcharge mechanism [5]

Another form of electrical abuse is external short circuit, which occurs when the positive and negative terminals of the battery are directly connected through a low-resistance path. This condition allows a very large current to flow through the cell in a short amount of time, generating significant heat due to ohmic losses. The rapid temperature increase can damage internal components, accelerate degradation reactions, and potentially trigger thermal runaway if the generated heat is not dissipated.

Overdischarge represents a third electrical abuse condition. When a battery is discharged below its minimum safe voltage, the copper current collector of the anode can begin to dissolve into the electrolyte. During subsequent charging cycles, the dissolved copper may redeposit inside the cell in the form of metallic filaments, which can pierce the separator and create internal short circuits.

Overall, electrical abuse conditions can compromise the structural integrity and electrochemical stability of the battery, leading to increased heat generation and raising the risk of thermal runaway. For this reason, modern battery systems are typically equipped with battery management systems (BMS) designed to monitor voltage, current, and temperature, preventing the cell from operating outside its safe electrical limits.

2.2.2 Thermal Abuse

Thermal abuse occurs when the battery is exposed to temperatures outside its safe operating range. This condition may result from external heating sources, malfunction of the thermal management system, exposure to high ambient temperatures, or heat transfer from neighboring cells in a battery module. When the temperature increases beyond the designed operating limits, the internal components of the battery begin to degrade, and a sequence of exothermic reactions can be triggered.

As the temperature rises, the first significant process is typically the decomposition of the Solid Electrolyte Interphase (SEI) layer on the surface of the graphite anode. This protective layer normally stabilizes the interface between the electrolyte and the electrode, but at elevated temperatures it becomes unstable and starts to decompose. The breakdown of the SEI exposes fresh electrode surface to the electrolyte, promoting additional exothermic reactions that generate further heat.

With further temperature increase, other components of the battery begin to degrade. The organic electrolyte may start to decompose, producing flammable gases and releasing heat. At the same time, the polymer separator can shrink or melt, potentially allowing direct contact between the anode and cathode. This can lead to internal short circuits, which

drastically increase the local current density and accelerate heat generation.

If the heat generated by these reactions cannot be dissipated efficiently, the temperature continues to rise until the cathode material becomes thermally unstable and begins to decompose. This process can release oxygen, which reacts with the electrolyte in highly exothermic reactions. At this stage, the system can rapidly enter thermal runaway, leading to a dramatic temperature increase and potentially causing venting, fire, or explosion.

Thermal abuse is therefore particularly dangerous because it can originate from external environmental conditions or from heat generated within the battery pack itself. For this reason, effective thermal management systems and accurate thermal modeling are essential to prevent the battery from reaching temperatures at which these destabilizing reactions begin to occur.

2.2.3 Mechanical Abuse

The third major triggering mechanism of Thermal Runaway in lithium-ion batteries is mechanical abuse, which occurs when the cell is subjected to physical damage or deformation. This type of abuse may result from impacts, crushing, penetration, vibration, or manufacturing defects, and it can compromise the structural integrity of the battery components.

Mechanical damage can directly affect the internal structure of the cell, particularly the separator that physically isolates the anode and cathode. If the separator is punctured, torn, or compressed due to external forces, the electrodes may come into direct contact, leading to an internal short circuit. This condition allows a large current to flow locally within the

cell, generating significant heat through resistive losses. Some work as “Multi-field interpretation of internal short circuit and thermal runaway behavior for lithium-ion batteries under mechanical abuse”[6] show as the porosity of the separator change with the compression strain, consequentially the effective resistance of the separator depends on how much the cell is damaged.

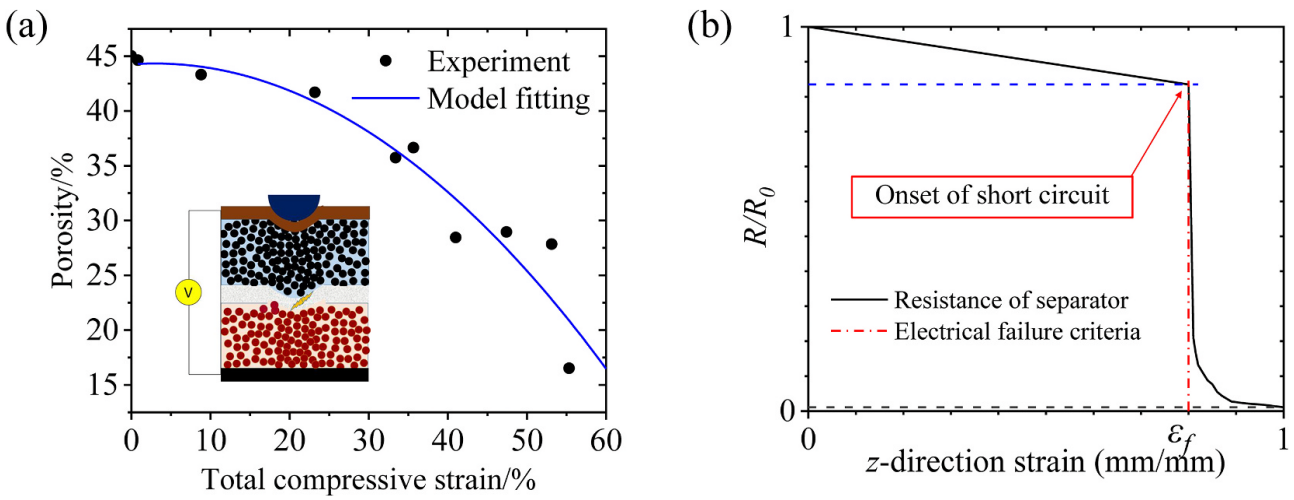

Figure 4 Porosity vs strain [6]

In addition to separator failure, mechanical deformation can also damage the electrode layers and the current collectors. The displacement or fracture of these components may create localized regions of high current density, further increasing heat generation. Moreover, mechanical stress can lead to cracks in the electrode materials, exposing fresh reactive surfaces to the electrolyte and potentially accelerating parasitic chemical reactions.

Another possible consequence of mechanical abuse is the rupture of the cell casing, which can result in electrolyte leakage and exposure of internal components to the external environment. Since the electrolyte

used in lithium-ion batteries is typically composed of flammable organic solvents, this situation increases the risk of ignition if sufficient heat or an external spark is present.

If the heat generated by internal short circuits and chemical reactions cannot be dissipated efficiently, the cell temperature may rise rapidly and trigger the sequence of reactions that lead to thermal runaway. Mechanical abuse is therefore particularly relevant in applications such as electric vehicles, where batteries may be exposed to severe stresses during accidents or collisions.

For this reason, significant efforts in battery design focus on improving the mechanical robustness of cells and battery packs, as well as implementing protective structures that can mitigate the effects of impacts or deformation, thereby reducing the likelihood of internal short circuits and improving overall system safety.

2.3 Exothermic Reactions and Runaway Sequence

At relatively low temperatures, typically below 80–90 °C, the battery experiences a gradual temperature increase mainly due to ohmic losses and normal electrochemical reactions. In this range, the cell can still operate in relatively stable conditions, provided that the generated heat is properly dissipated through an effective thermal management system.

When the temperature rises above approximately 90–120 °C, the first signs of instability begin to appear. In this stage, the decomposition of the Solid Electrolyte Interphase (SEI) layer occurs on the surface of the negative electrode. The breakdown of this protective layer leads to exothermic reactions between the electrolyte and the graphite anode,

generating additional heat and accelerating the increase in cell temperature.

As the temperature reaches the range of about 130–200 °C, more critical processes take place. In particular, the polymer separator that physically isolates the anode and cathode may start to melt or shrink. The loss of separator integrity can lead to internal short circuits, which cause localized current spikes and further heat generation. At the same time, the electrolyte and electrode materials begin to undergo decomposition reactions, releasing gases and additional thermal energy.

When the temperature exceeds approximately 200–250 °C, the system enters the actual thermal runaway phase. At this stage, cathode material starts to decompose, often releasing oxygen. This oxygen can react with the highly flammable organic electrolyte, producing strong exothermic reactions that rapidly increase both temperature and internal pressure. The temperature can rise dramatically within a very short time.

In the final stage, temperatures may reach values above 600–800 °C depending on the battery chemistry. A large amount of gas generated inside the cell can cause venting, ignition, or even explosion. In battery packs composed of multiple cells, the heat released during thermal runaway can also propagate to neighboring cells, triggering a chain reaction known as thermal runaway propagation.

Understanding the different stages of thermal runaway is essential for improving battery safety and for developing reliable thermal models. A detailed knowledge of the mechanisms responsible for heat generation and of the temperature thresholds that trigger these reactions allows researchers to design safer battery systems and to develop predictive tools

for assessing potential failure conditions in lithium-ion battery applications.

2.4 Effects and Consequences on the Cell

When Thermal Runaway occurs, the electrochemical and structural integrity of the cell is severely compromised. The sequence of exothermic reactions and the rapid increase in temperature lead to significant changes in the electrical behavior of the battery, as well as to permanent damage to its internal components.

One of the most immediate electrical consequences of thermal runaway is a sudden drop in the cell voltage. This behavior is mainly caused by the occurrence of internal short circuits and the degradation of the electrode materials. As the separator melts or shrinks and the electrodes come into contact, a low-resistance internal pathway is created, which rapidly discharges the stored energy of the battery.

From an electrochemical perspective, the effective State of Charge (SOC) of the cell quickly decreases as the stored lithium is consumed through uncontrolled reactions and internal current flows. In many cases, the cell experiences an almost complete and uncontrolled discharge during the runaway event. However, the resulting SOC after the event is often difficult to determine precisely because the electrochemical structure of the electrodes may be permanently altered.

After a thermal runaway event, the battery cell is generally considered irreversibly damaged and cannot be safely reused. The extreme temperatures reached during the event can cause severe degradation of the electrodes, decomposition of the electrolyte, melting of the separator,

and deformation or rupture of the cell casing. These processes lead to a permanent loss of the electrochemical functionality of the cell.

Even if the cell does not completely ignite or explode, internal materials may have undergone structural changes that compromise their stability and safety during future operation. For this reason, cells that have experienced thermal runaway are typically classified as hazardous waste and must be handled and disposed of following appropriate safety procedures.

Another important consequence of thermal runaway is the release of gases and volatile compounds produced by the decomposition of the electrolyte and electrode materials. Lithium-ion batteries typically contain organic carbonate-based electrolytes that can decompose at high temperatures, generating flammable gases such as carbon monoxide, carbon dioxide, methane, and hydrogen.

In addition to these gases, toxic compounds may also be released. For example, the decomposition of lithium salt electrolytes can produce Hydrogen Fluoride (HF), a highly corrosive and toxic gas that poses serious health risks if inhaled. Exposure to these gases can cause respiratory irritation, chemical burns, and other health hazards for humans, making thermal runaway events particularly dangerous in confined environments.

Furthermore, the combustion of battery materials can release fine particulate matter and metal-containing compounds into the surrounding environment, which may also represent potential health risks.

In practical applications, individual cells are rarely used alone but are typically assembled into modules and larger battery packs. In these systems, a thermal runaway event occurring in a single cell can have serious consequences for the entire battery system.

The large amount of heat released during thermal runaway can transfer to neighboring cells through conduction, convection, and radiation. If adjacent cells reach their critical temperature thresholds, they may also enter thermal runaway [7], triggering a chain reaction known as thermal runaway propagation. This phenomenon can lead to the failure of an entire module or battery pack.

At the system level, such events can cause extensive damage to the battery housing, electrical connections, and surrounding components. In applications such as electric vehicles or stationary energy storage systems, thermal runaway propagation can result in large-scale fires that are difficult to control due to the sustained release of energy and flammable gases.

For these reasons, preventing the initiation and propagation of thermal runaway is a key objective in the design of modern battery systems. Effective thermal management, robust mechanical protection, and advanced monitoring systems are essential to mitigate the risks associated with this phenomenon and to ensure the safe operation of lithium-ion batteries in large-scale applications.

3. Physical Modeling of the Battery

3.1 State of Art of Thermal Runaway Model

The thermal runaway phenomenon in lithium-ion batteries has been widely investigated through the development of mathematical models of varying complexity, with the aim of understanding and predicting the onset and propagation of thermal instability within the cell. Early modeling approaches were primarily based on simplified thermal or electro-thermal formulations, in which the temperature evolution of the cell was described through global energy balances. In these models, heat generation was typically represented through empirical kinetics associated with the exothermic decomposition reactions of the battery components. In particular, reactions such as the decomposition of the solid electrolyte interphase (SEI), electrolyte reactions with the anode, and cathode decomposition were often described using Arrhenius-type expressions. Several pioneering studies adopted this approach to investigate the abuse behavior of lithium-ion cells and the conditions leading to thermal runaway. Among the most notable contributions are the thermal models developed by Hatchard et al. (2001)[8], as well as the abuse behavior studies by Spotnitz and Franklin (2003)[9], which introduced reaction-based heat generation terms to simulate the thermal response of lithium-ion batteries under critical conditions. Similar approaches have also been employed in more recent studies, such as the work by Coman et al. (2017)[10], where thermal runaway triggered by internal short circuits was investigated through coupled electro-thermal modeling. While these models were able to qualitatively reproduce the rapid temperature rise associated with runaway conditions, they generally lacked a detailed description of the electrochemical processes occurring inside the cell.

For this reason, more recent research has increasingly focused on the development of multi-physics models that combine electrochemical and thermal phenomena to provide a more comprehensive representation of battery behavior. Among the most widely adopted electrochemical frameworks is the “pseudo-two-dimensional (P2D) model” developed by Doyle, Fuller, and Newman[11], which has become a standard approach for lithium-ion battery simulations. This model describes lithium transport in the electrolyte along the thickness of the cell while simultaneously accounting for lithium diffusion within the solid particles of the electrodes. As a result, it captures the key electrochemical mechanisms governing battery operation while maintaining a manageable computational cost. In models aimed at studying thermal runaway, the P2D formulation is typically coupled with a thermal model describing heat generation and dissipation within the cell. A key feature of these approaches is the presence of a bidirectional coupling between temperature and heat generation: on one hand, temperature affects electrochemical properties and reaction kinetics, such as diffusion coefficients, conductivity, and reaction rates; on the other hand, electrochemical reactions and irreversible losses generate heat that influences the temperature distribution within the battery. This electro-thermal coupling allows for a more realistic representation of battery behavior under critical conditions and plays a crucial role in capturing the mechanisms that may ultimately lead to the onset of thermal runaway. The model adopted in this work follows this approach, combining a P2D electrochemical formulation with a bidirectional coupling between the thermal and electrochemical domains in order to consistently capture the

interaction between heat generation and temperature evolution during battery operation.

3.2 Modeling Approach

This model is structured as a bidirectionally coupled interaction between two distinct sets of equations. The first block describes the electrochemical model and includes the equations governing the main electrochemical variables, namely the electric potentials, the reaction current density, the species concentrations, and the heat generated during normal battery operation. To solve these equations, a one-dimensional geometry is adopted, as it provides a reasonable approximation of the real physical processes while avoiding an excessive increase in computational complexity and the number of degrees of freedom.

The second block represents the thermal model. In this case, a two-dimensional axisymmetric geometry is used in order to compute the temperature distribution throughout the battery domain. This block also accounts for the heat generated by temperature-dependent Arrhenius reactions.

The two models are strongly coupled and exchange their main quantities: the electrochemical model provides the heat generation term $Q$to the thermal model, while the thermal model returns the temperature T, which influences the electrochemical processes. As a result, the behaviour of the system emerges from the mutual interaction between the electrochemical and thermal domains.

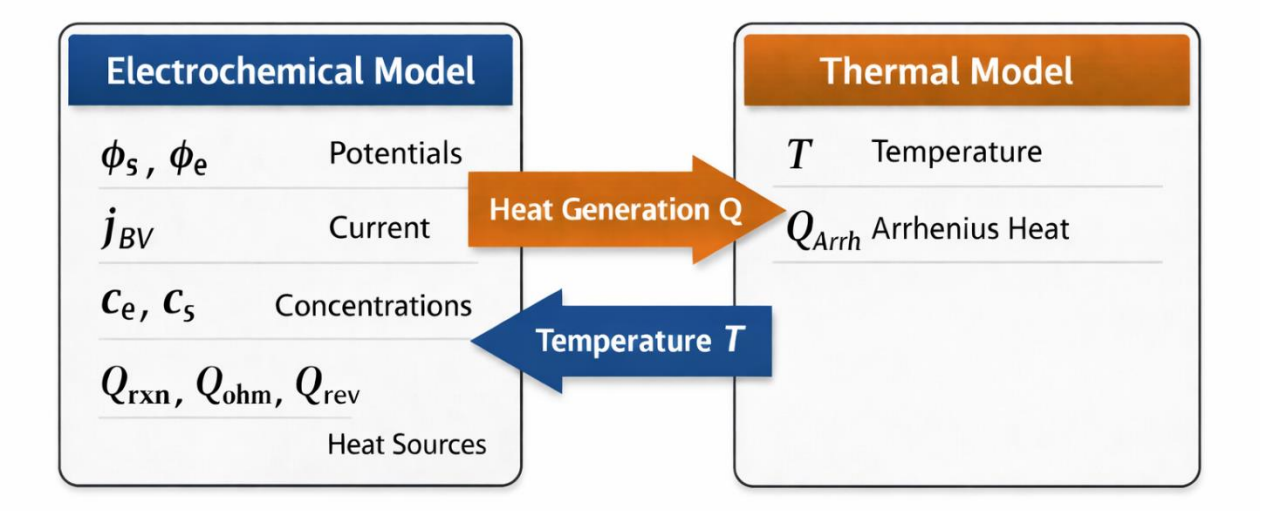

Figure 5 Blocks Model [AI generated]

3.3 Electrochemical Model

3.3.1 Porous Electrode Theory

Electrodes used in lithium-ion batteries are not continuous solid structures but are instead composed of a large number of small particles. This heterogeneous morphology is intentionally designed to increase the effective surface area available for electrochemical reactions. By enlarging the interfacial area between the active material and the electrolyte, lithium transport is facilitated and the internal resistance of the cell is reduced, which ultimately improves the power and energy delivery capability of the battery. An example of this microstructure can be observed in scanning electron microscope images of graphite electrodes, where the granular nature of the material is clearly visible.

Modeling such a complex structure at the particle scale would require extremely high computational resources. To overcome this limitation, the

porous electrode theory introduced by Newman [11] provides a simplified framework in which the heterogeneous electrode is treated as a homogenized medium. Within this approach, the transport equations governing ionic and electronic motion retain the same general form as the classical conservation equations, but their parameters are modified to account for the porous nature of the medium.

In this formulation, the porous electrode is considered as a domain where solid active material and liquid electrolyte coexist. Instead of explicitly resolving each particle, the system is represented through an averaged description of the two phases. At every location within the electrolyte phase, the model assumes the presence of a representative spherical active material particle with radius R. Lithium ions moving through the electrolyte can either continue diffusing in the liquid phase or intercalate into the solid particle.

The concept of a pseudo-dimension is introduced in porous electrode models to represent the diffusion of lithium inside the active material particles without explicitly resolving the full three-dimensional microstructure of the electrode. In reality, each electrode is composed of a large number of solid particles surrounded by electrolyte, and lithium ions can intercalate into these particles during battery operation. Modeling every particle and its geometry would require an extremely fine spatial discretization and a very large computational cost. To avoid this, the porous electrode theory adopts a homogenized description of the electrode while still retaining the essential physics of lithium diffusion inside the solid phase.

In this framework, each point of the macroscopic electrode domain is associated with a representative spherical particle of active material. The

lithium concentration within this particle is not assumed to be uniform, but varies along the particle radius. For this reason, an additional spatial coordinate is introduced, corresponding to the radial direction inside the particle. This coordinate does not represent a real spatial dimension of the electrode domain but rather an internal coordinate describing transport inside the particle, and it is therefore referred to as a pseudo-dimension.

The diffusion of lithium in the solid phase is then modeled as a one-dimensional diffusion process along this radial coordinate, from the center of the particle to its surface. The surface of the particle is coupled with the electrolyte through the electrochemical reaction current density, which determines the flux of lithium entering or leaving the particle. In this way, the pseudo-dimension allows the model to capture the internal diffusion limitations of the active material while keeping the overall computational complexity manageable.

3.3.2 Electrochemical Equation

The equations for the electrochemical model are taken from the work of Tiuterev Mikhail Ivanovich: “Analysis of numerical models describing the aging of lithium-ion batteries due to the formation of an interphase layer of solid electrolyte” [12].

1) Law of conservation of mass in solid body

$$\frac{\partial c_s}{\partial t}(r,x,t) = D_s \Delta c_{s(r,x,t)} = \frac{1}{r^2}\frac{\partial}{\partial r}\left(D_s r^2 * \frac{\partial c_s}{\partial r}\,(r,x,t)\right) \qquad (1)$$

The variation of the concentration of li-ions in the positive and negative electrode is represented by the diffusion equation. This equation describes as the lithium moves along the solid particle, during charge ions enter in the negative while during discharge the cathode is fulfilled to its maximum capacity.

c_s is the concentration of Li inside the solid; D_s is the diffusion coefficient (temperature dependent); r is the coordinate of the particle implemented as pseudo dimension.

The conditions at the boundary are:

$$\frac{\partial c_s}{\partial r}(r = 0, x, t) = 0$$

$$\frac{\partial c_s}{\partial r}(r = R_s, x, t) = -j(x, t)$$

It shows how the butler volmer current is imposed at the external radius in a way we respect the balance of mass between electrolyte and solid.

2) Law of conservation of mass in electrolyte

$$\frac{\partial}{\partial t}\left(\varepsilon_e c_e(x,t)\right) + \nabla\left(-D_e^{eff}\nabla c_e(x,t)\right) = (1 - t_+^0)a_s j(x,t) \qquad (2)$$

This equation describes how Li-ions move in the electrolyte. It represents a balance between the litihium that moves from anode to cathode and lithium consumed/generated by reaction.

ε_e is the porosity of the electrolyte, c_e is the concentration in the electrolyte, D_e^{eff} is the effective diffusion coefficient.

t_+^0 is the transport number of lithium ions; in other words, it is the fraction of the total current which is transported by lithium ions, the other part is transported bi anions.

In this work the electrolyte is assumed to be electrically neutral, and so:

$$c_e(x,t) = c_+(x,t) = c_-(x,t)$$

This means that the total amount of lithium remains constant.

In porous electrode models, transport processes occurring in the electrolyte phase are not described using the intrinsic transport properties of the pure electrolyte, but rather through effective transport coefficients. This approach is necessary because the electrolyte inside a battery electrode does not occupy a free and homogeneous volume. Instead, it is distributed within a complex porous structure formed by the solid active material, conductive additives, and binder. As a consequence, the pathways available for ionic transport are restricted and highly tortuous compared to a bulk liquid electrolyte.

If the intrinsic diffusivity of the electrolyte were used directly in the governing equations, the model would overestimate the rate of ion transport because it would implicitly assume that lithium ions move through a straight and unobstructed medium. In reality, ions must move

through narrow pores and around solid particles, which increases the effective path length and reduces the overall transport rate. To account for these geometric constraints, the transport coefficients are corrected to obtain effective properties that represent the averaged behavior of the porous medium.

The most common approach used in porous electrode theory is the Bruggeman correction, which modifies the transport coefficients according to the porosity of the electrode. In this formulation, the effective diffusivity of lithium ions in the electrolyte is expressed as

$$D_{eff} = D\varepsilon^{brug}$$

where D is the intrinsic diffusivity of the electrolyte, ε is the porosity (the fraction of the volume occupied by electrolyte), and brug is the Bruggeman exponent, typically assumed to be around 1.5 for battery electrodes.

This empirical relation accounts for the increased tortuosity of the ionic pathways within the porous structure. As the porosity decreases, the available cross-sectional area for ion transport becomes smaller and the pathways become more convoluted. The Bruggeman correction therefore reduces the effective diffusivity to reflect the additional resistance encountered by ions as they move through the porous medium.

The same concept is applied to other transport properties, such as the ionic conductivity of the electrolyte and the electronic conductivity of the solid phase, which are also expressed in effective form when used in porous electrode models. By introducing these effective parameters, the model

can capture the influence of the electrode microstructure on transport phenomena without explicitly resolving the detailed geometry of the porous network. This approach significantly simplifies the computational problem while still preserving the essential physical behaviour of the system.

The condition at the boundary is:

$$\frac{\partial c_e}{\partial x}(x = 0, t) = \frac{\partial c_e}{\partial x}(x = L_{tot}, t) = 0$$

3) Law of conservation of charge in the solid phase

$$\nabla\left(-\sigma^{eff}\nabla\varphi_s(x,t)\right) = -a_{as}Fj(x,t) \qquad (3)$$

The variation of the electrical potential is linked to the Butler Volmer current, multiplied for the specific surface area $a_{as} = \frac{A}{V_{electrode}}$. In porous electrode theory, the electrochemical reaction rate is typically described by the Butler–Volmer equation, which provides the reaction current density i_{BV} per unit interfacial area between the solid active material and the electrolyte, with units of $[A/m^2]$. However, the conservation equations used to describe charge transport in porous

electrodes are formulated over a representative control volume of the electrode and therefore require source terms expressed per unit volume $[A/m^3]$. To bridge this difference in scale, the Butler–Volmer current density is multiplied by the specific surface area a_s, defined as the total interfacial area between the solid phase and the electrolyte per unit volume of electrode. The quantity $a_s$therefore converts a surface-based reaction rate into a volumetric source term that can be consistently included in the charge conservation equations. Physically, this parameter accounts for the fact that electrochemical reactions occur on the surfaces of numerous active material particles distributed throughout the porous electrode. As a result, the total reaction current generated within a given electrode volume depends not only on the local interfacial kinetics but also on the amount of available reaction surface. For electrodes composed of spherical particles, the specific surface area can be approximated as $a_s = 3\varepsilon_s/R_p$, where $\varepsilon_s$is the volume fraction of active material and $R_p$is the particle radius, highlighting how smaller particles increase the available interfacial area and therefore the volumetric reaction rate.

The boundary conditions are:

$$\sigma_{eff} * \frac{\partial \varphi_s}{\partial x}(x = 0, t) = -i(t)$$

$$\varphi_s(x = L_{tot}, t) = 0$$

How the first condition shows, at the positive electrode is imposed a current to simulate charge and discharge.
At the negative is assigned a ground potential in order to define a reference for the electric potential field. The governing equations for charge conservation in both the solid and electrolyte phases determine only potential differences, not absolute potential. As a result, without

fixing the potential at one point in the domain, the system of equations would have infinitely many equivalent solutions differing by an arbitrary constant offset. Imposing a ground condition (usually $\phi = 0$) at one electrode removes this indeterminacy and ensures a unique numerical solution. Physically, this does not affect the behavior of the system, because electrochemical processes such as charge transfer and overpotential depend only on potential differences between phases, not on the absolute value of the potential itself. Therefore, grounding one electrode simply establishes a convenient reference level for the electric potential while preserving the correct physics of the electrochemical reactions and current distribution within the cell.

4) Law of conservation of charge in electrolyte

$$\nabla\left(-k^{eff}\nabla\varphi_e(x,t) - k_d^{eff}\nabla \ln c_e\,(x,t)\right) = a_s F j(x,t) \qquad (4)$$

On the left of this equation we have two members, the first one takes into account the ionic migration in the electric field, the second term is given by the diffusion due to the concentration gradient

$$k_d = \frac{2kRT}{F}\left(1 + \frac{\partial \ln f_{+-}}{\partial \ln c_e}\right)(t_+^0 - 1)$$

The conditions at the borders are:

$$\frac{\partial \varphi_e}{\partial x}(x = 0, t) = \frac{\partial \varphi_e}{\partial x}(x = L_{tot}, t) = 0$$

5) Butler Volmer equation

$$j(x,t) = \frac{i_0}{F}\left(\exp\left(\frac{(1-\alpha)F}{RT}\eta(x,t)\right) - \exp\left(-\frac{\alpha F}{RT}\eta(x,t)\right)\right) \qquad (5)$$

Where:

$i_0 = Fk_{0,norm}\left(\frac{c_e}{c_{e0}}\right)^{1-\alpha}\left(\frac{c_{s,max}-c_{s,e}}{c_{s,max}}\right)^{1-\alpha}\left(\frac{c_{s,e}}{c_{s,max}}\right)^{\alpha}$ is the exchange current density

$eta = \eta = \varphi_s - \varphi_e - U_{eq}$ is the overvoltage

The Butler Volmer equation expresses the local reaction current density as a function of the electrochemical overpotential and represents the kinetics of charge transfer across the electrode–electrolyte interface. Physically, the Butler–Volmer formulation accounts for the fact that both oxidation and reduction reactions can occur simultaneously at the interface.

Greater will be the potential difference with respect to the equilibrium, faster will be the reaction.

6) Lithium conservation

$$Li_{tot} = cs_{max,pos} V_{pos} \theta_{pos} + cs_{min,neg} V_{neg} \theta_{neg} + ceVe \qquad (6)$$

Is possible to recognize the maximal quantity of Li-ions that can be intercalated inside the electrodes (cs), the volume occupied by electrodes and electrolyte (V and Ve which are dependent on porosity) and finally the utilization factor θ.

The utilization factor is the percentage of lithium intercalated with respect with the maximum quantity. For the anode, it is assumed a full range for the utilization factor (0-100%), while for the positive electrode made of NMC is assumed a range of (0.15-0.9%) [27]. This limitation is mainly related to electrochemical and structural stability constraints of the cathode material. At very low lithium concentrations (i.e., under strong delithiation conditions), the NMC structure can become structurally unstable, leading to phenomena such as crystal lattice collapse, oxygen release, and increased reactivity with the electrolyte. On the other hand, lithium fractions close to full lithiation may promote material degradation, mechanical stress within the particles, and loss of reaction reversibility.

Fundamental properties depending on the quantity of ions inside the electrode are the equilibrium potential and entropic potential; the utilized curve for both are reported below.

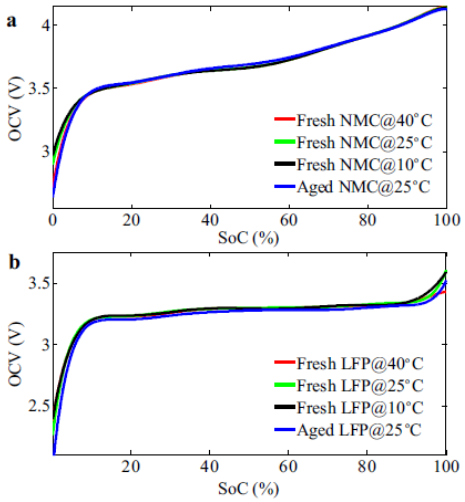

Figure 6 Equilibrium Potential for cathode NMC[28]

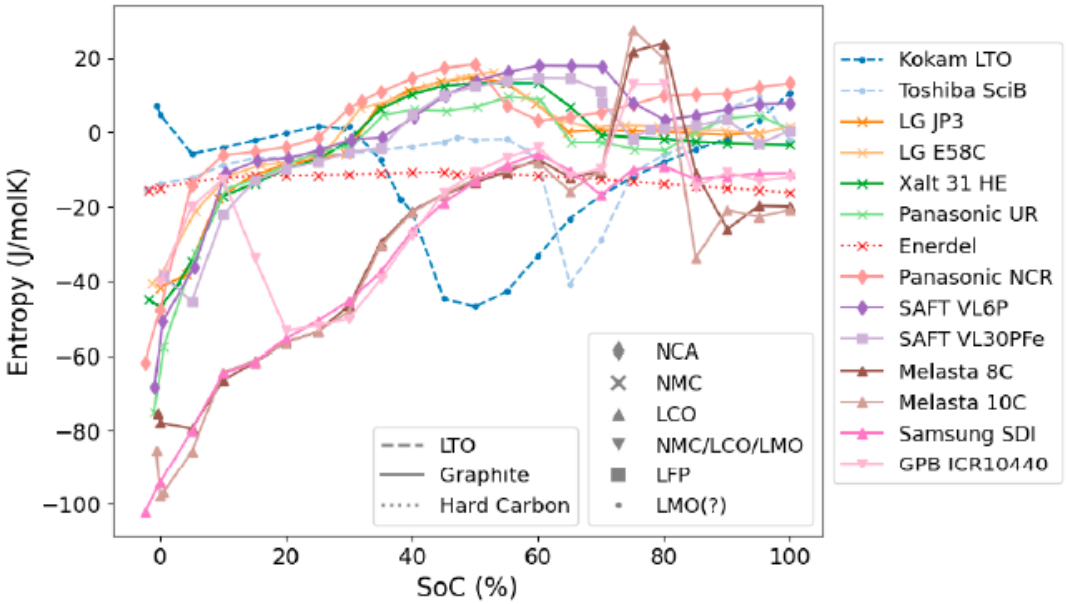

Figure 7 Entropy potential [29]

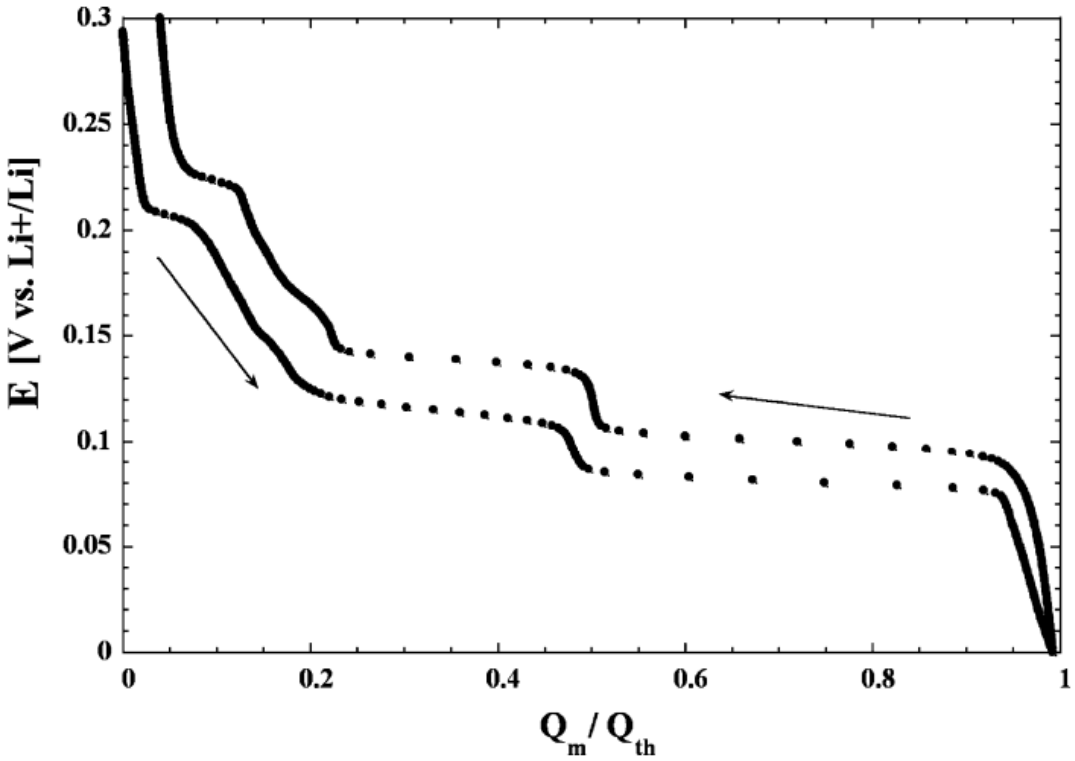

Figure 8 Equilibrium Potential for Grafite Anode[14]

7) Reversible heat

$$Q_{rev} = F a_{as} J_{bv} * \frac{\partial U_{pos}}{\partial T} \left(\frac{cs}{cs_{max}}\right) T_{ref} \qquad (7)$$

This contribute of the heat is directly dependent on the Temperature of the cell and the entropic potential.
The sign of it is linked to the sign of entropic potential; during discharge if it is greater than 0 the heat will be positive and so the reaction absorb heat, on the other case if the entropic potential is less than 0 the heat will be negative and the reaction release heat. For the process of charge is the

opposite.

During short circuit, this term is the less relevant respect to the others.

8) Irreversible heat

$$Q_{rnx} = F * a_{as} J_{bv} \eta \qquad (7)$$

The overpotential represents the extra potential required to overcome kinetic limitations of the electrochemical reaction.

The presence of this overpotential leads to irreversible heat generation at the electrode–electrolyte interface. Physically, this heat corresponds to the portion of electrical energy that cannot be converted into useful electrochemical work and is instead dissipated as thermal energy. During short circuit, it plays a fundamental role.

9) Ohmic heat

$$Q_{ohm} = \sigma_{eff} * \left(\frac{\partial \varphi_s}{\partial x}\right)^2 + k_{eff} * \left(\left(\frac{\partial \varphi_e}{\partial x}\right)^2 - \frac{k_d}{c_e} * \frac{\partial c_e}{\partial x} * \frac{\partial \varphi_e}{\partial x}\right) \qquad (7)$$

The first term on the right take in account the ohmic heat due to conductivity in the solid, the second term is for the conductivity of ions of electrolyte and there is also a diffusion term due to the concentration gradient: part of the energy is not dissipated as heat but is linked to the chemical work and so reduce the total heat generated. During short circuit this term is the most relevant.

3.4 Thermal Model

The thermal behavior of the cell is described using a two-dimensional axisymmetric model. The axisymmetric formulation is appropriate for this type of spirally wound battery because heat conduction along the spiral direction is typically negligible. Instead of explicitly resolving heat transfer across each individual layer of the jelly-roll structure—such as the positive electrode, separator, and negative electrode—the entire wound stack is represented as a single equivalent domain corresponding to the active battery material. This homogenized representation significantly simplifies the model while still capturing the dominant heat transport mechanisms. Previous studies have demonstrated that such assumptions provide an accurate description of the thermal response of spiral-wound cells when heat is removed primarily through natural convection [15,16].

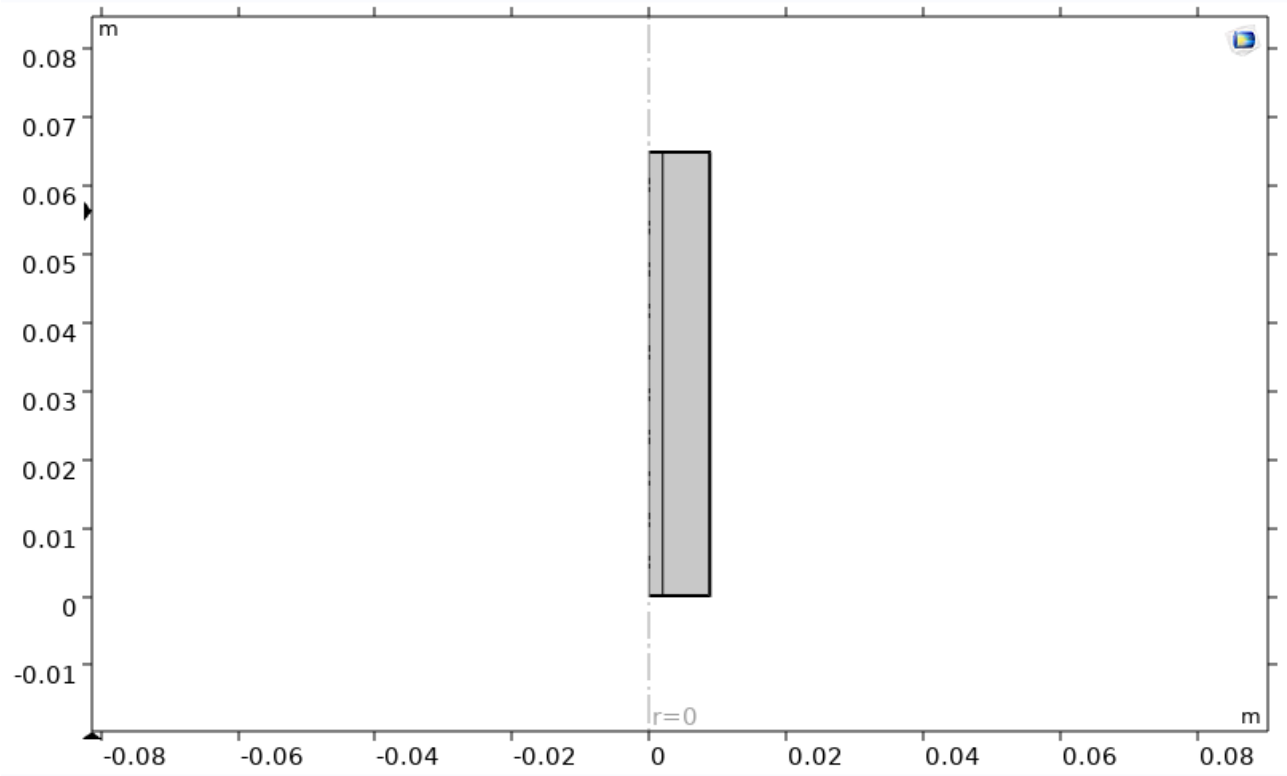

Figure 9 Geometry of thermal model

The geometry consists of three domains:

1)Battery canister

2)Active battery material (wound sheets of cell material)

3)Mandrel (isolator around which the battery cell sheets are wound)

The properties are taken from the work of Hossein Maleki [17]; density and specific heat in the paper are not referred to a porous material and so are manipulated as follows to have the correct value:

$$\rho_{eff} = (1 - \varepsilon)\rho_{solid} + \varepsilon\rho_{elec}$$

Where ρ_{solid} is the value of the non-porous material and ε is the porosity.

$$Cp_{eff} = \left((1-\varepsilon)Cp_{solid} + \varepsilon\rho_{elec}Cp_{elec}\right)/\rho_{eff}$$

As is shown in the Comsol guide [18] for the fact that the active battery material is assumed to consists of one or several battery cells wound spirally into a cylinder, the thermal conductivities are anisotropic, with higher value along the cylinder length direction than in the radial direction [15].

$$k_{t_r} = \frac{\sum L_i}{\frac{\sum L_i}{k_{T_i}}}$$

$$k_{T_{ang}} = \frac{\sum L_i k_{T_i}}{\sum L_i}$$

Where i indicates different layers (anode, cathode, electrolyte).

In a similar way, density and specific heat are calculated for the active battery material.

$$\rho_{batt} = \frac{\sum L_i \rho_i}{\sum L_i}$$

$$C_{p,batt} = \frac{\sum L_i \rho_i C_{p_i}}{\sum L_i \rho_i}$$

The main equation solved in the thermal model is the energy conservation:

$$\rho Cp * \frac{\partial T}{\partial t} = \nabla(k\nabla T) + Q_{tot} \qquad (8)$$

Where the left-hand side represents the accumulation of thermal energy within the material, while the right-hand side includes the heat transport and heat generation mechanisms.

The first term,

$$\rho C_p \frac{\partial T}{\partial t},$$

represents the temporal variation of the internal thermal energy of the system. This term accounts for the accumulation or depletion of heat within the battery over time.

The second term,

$$\nabla \cdot (k \nabla T),$$

describes heat transfer by conduction, according to Fourier's law. The parameter $k$is the thermal conductivity of the material and determines how heat propagates from regions of higher temperature to regions of lower temperature inside the cell.

Finally, the term Q is the sum of different contribution:

1) The electrochemical heating sources that we have defined in the electrochemical model: Reversible heat, ohmic heat, irreversible heat.
2) The heat dissipation that takes into account both convection and radiation

$$Q_{conv} = h(T_{amb} - T)$$

$$Q_{rad} = \epsilon\sigma(T_{amb}^4 - T^4)$$

By solving the energy conservation equation, it is possible to determine the spatial and temporal temperature distribution within the battery cell, which is essential for analyzing performance limitations, degradation mechanisms, and, in critical conditions, the onset of thermal runaway.

In failure situations, the last term of the energy conservation equation has to include other two terms: the heat generated by short circuit and the heat generated by thermal decomposition of electrodes and electrolyte.

$$Q_{tot} = (Q_{rev} + Q_{rnx} + Q_{ohm}) + (Q_{conv} + Q_{rad}) + Q_{sc} + Q_{arr} \quad (9)$$

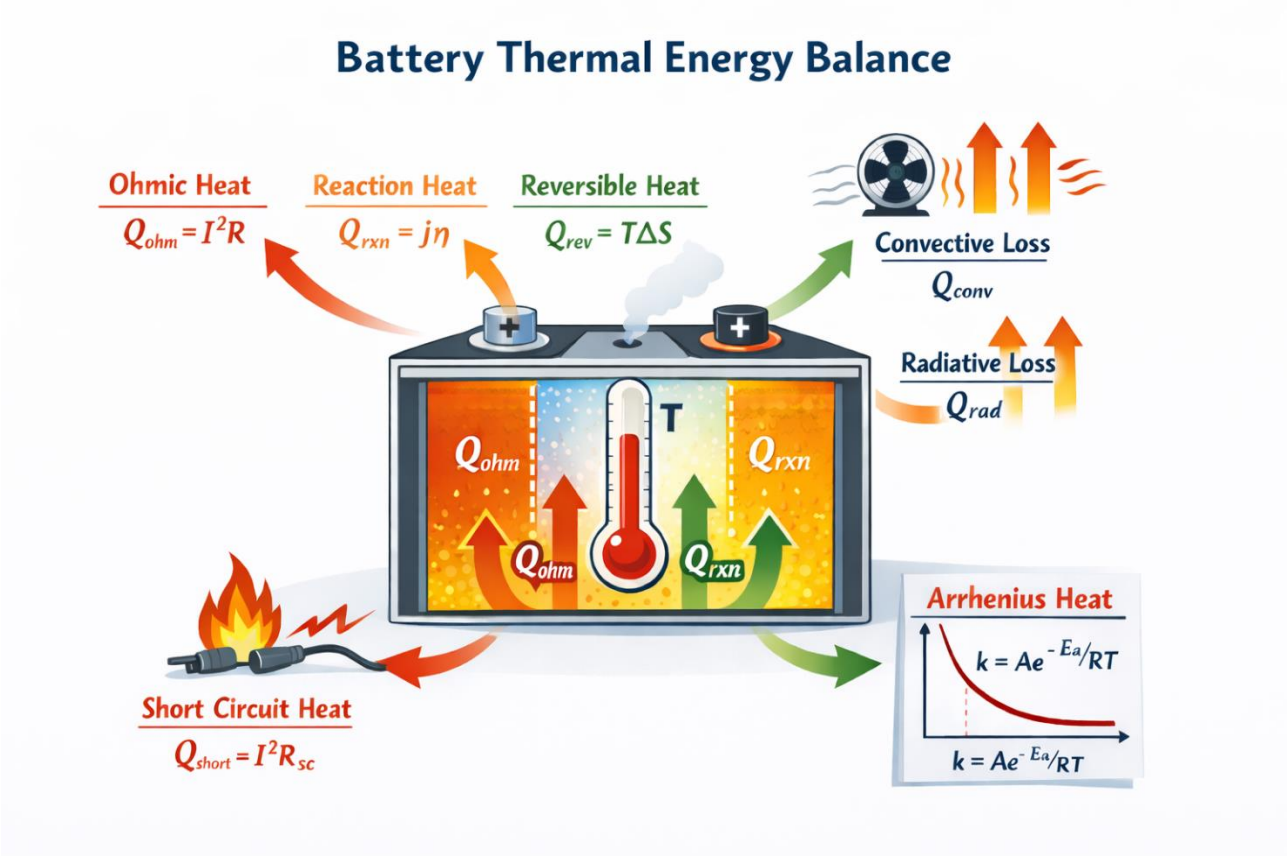

Figure 10 Battery Thermal Energy Balance [Ai generated]

3.4.1 Arrhenius Heat

In the context of lithium-ion battery thermal modeling, Arrhenius heat generation refers to the heat released by exothermic chemical reactions whose rate follows an Arrhenius-type temperature dependence. These reactions typically involve the decomposition of battery components such as the solid electrolyte interphase (SEI), the reaction between the electrolyte and the electrodes, and the decomposition of the cathode material at elevated temperatures. The rate of these reactions can be expressed through the Arrhenius law,

$$k = A \exp\left(-\frac{E_a}{RT}\right)$$

where $A$is the pre-exponential factor, $E_a$is the activation energy of the reaction, $R$is the universal gas constant, and $T$is the temperature. Because the reaction rate increases exponentially with temperature, even a small rise in temperature can significantly accelerate these exothermic reactions, leading to additional heat generation within the cell. This mechanism is particularly important in the study of thermal runaway, since it introduces a positive feedback loop: increasing temperature accelerates chemical reactions, which generate more heat and further increase the temperature. Incorporating Arrhenius-type heat sources in thermal models therefore allows the prediction of the onset and propagation of thermal runaway, enabling a more accurate description of the self-heating behavior and the safety limits of lithium-ion batteries.

In particular, the reaction used in this work are taken from “Multi-field interpretation of internal short circuit and thermal runaway behavior for lithium-ion batteries under mechanical abuse” [6]

1) SEI decomposition

$$\frac{dc_{sei}}{dt} = -A_{sei} \exp\left(-\frac{E_{a,sei}}{RT}\right) c_{sei} \qquad (10)$$

$$Q_{sei} = H_{sei} W_c A_{sei} \exp\left(-\frac{E_{a,sei}}{RT}\right) c_{sei} \qquad (11)$$

The first reaction corresponds to the decomposition of the solid electrolyte interphase (SEI) layer formed on the surface of the graphite

anode during battery operation. The SEI is thermodynamically unstable at elevated temperatures and begins to decompose typically between 80 °C and 120 °C. This reaction represents the initial stage of thermal runaway.

The decomposition of the SEI layer exposes fresh anode material to the electrolyte, enabling further parasitic reactions and accelerating heat generation within the cell. Although the heat released during SEI decomposition is relatively moderate compared to other reactions, it plays a critical role in initiating the thermal instability process.

2) Anode-decomposition

$$\frac{dz}{dt} = A_{ae} \exp\left(-\frac{z}{z_0}\right) \exp\left(-\frac{E_{a,ae}}{RT}\right) c_{ae} \quad (12)$$

$$\frac{dc_{ae}}{dt} = -A_{ae} \exp\left(-\frac{z}{z_0}\right) \exp\left(-\frac{E_{a,ae}}{RT}\right) c_{ae} \quad (13)$$

$$Q_{ae} = H_{ae} W A_{ae} \exp\left(-\frac{z}{z_0}\right) \exp\left(-\frac{E_{a,ae}}{RT}\right) c_{ae} \quad (14)$$

Once the SEI layer has degraded, the graphite anode becomes directly exposed to the electrolyte. At elevated temperatures, the lithiated graphite reacts with the organic electrolyte solvents, producing additional heat and gaseous species.

This reaction is typically more energetic than the SEI decomposition and contributes significantly to the temperature increase inside the cell. The rate of this reaction depends strongly on temperature and on the amount of active material still available for reaction, for this reason the variable z is introduced to take into account the fraction of electrolyte consumed. The heat generated during this stage further accelerates the overall thermal runaway process.

3) Cathode-decomposition

$$\frac{d\alpha}{dt} = A_{ce}\alpha \exp\left(-\frac{E_{a,ce}}{RT}\right) \quad (15)$$

$$Q_{ce} = H_{ce}W_p A_{ce}\alpha \exp\left(-\frac{E_{a,ce}}{RT}\right) \quad (16)$$

At higher temperatures, the cathode material undergoes structural decomposition. In batteries using cathode materials such as Nickel Cobalt Aluminum Oxide, thermal instability of the layered crystal structure leads to the release of oxygen from the lattice.

The released oxygen reacts with the electrolyte, producing highly exothermic reactions that dramatically increase the heat generation rate. This stage is often responsible for the most violent phase of thermal runaway, as both the decomposition of the cathode and the subsequent oxidation of electrolyte contribute to rapid temperature escalation.

The decomposition reaction is typically characterized by a relatively high activation energy, meaning that it becomes significant only once the temperature has already risen due to earlier reactions.

4) Electrolyte decomposition

$$\frac{dc_e}{dt} = -A_e \exp\left(-\frac{E_{a,e}}{RT}\right) c_e \quad (17)$$

$$Q_{ed} = H_e W_e = -A_e \exp\left(-\frac{E_{a,e}}{RT}\right) c_e \quad (18)$$

The final reaction considered in the thermal model is the decomposition of the electrolyte itself. At sufficiently high temperatures, the organic

carbonate solvents that compose the electrolyte begin to break down and react with other battery components.

Electrolyte decomposition releases additional heat and gaseous products, which can contribute to pressure buildup inside the cell. Although this reaction usually occurs after other degradation mechanisms have already started, it further amplifies the thermal runaway process and contributes to the overall energy released during the event.

Together, these four reactions describe the sequential degradation mechanisms that occur during thermal runaway. The SEI decomposition initiates the instability, the anode–electrolyte reaction accelerates heat generation, the cathode decomposition produces oxygen and large amounts of heat, and the electrolyte decomposition further intensifies the exothermic process. Modeling these reactions using Arrhenius-type kinetics allows the temperature-dependent behavior of the battery to be captured and enables the prediction of thermal runaway propagation within the cell.

Variable	c_{sei}	c_{ae}	z	α	c_e
Initial value	0.15	0.75	0.033	0.04	1

Table 1 Initial Values for Arrhenius [6]

The values for the constant of Arrhenius equation are taken from "Thermal Runaway propagation behaviour within 18,650 lithium-ion battery packs: A modelling study" [19] and are listed in the table below.

parameter	Sei-decomposition	Anode-decomposition	Cathode-decomposition	Electrolyte-decomposition
H [J/g]	/	/		155
W [kg/m^3]	/	/		$4.069e^{2}$
H*W [J/m^3]	$6.5763e^{7}$	$7.3410e^{7}$	$2.06e^{7}$	/
A [1/s]	$1.14e^{14}$	$7.18e^{13}$	$6.67e^{13}$	$5.14e^{25}$
E [J/mol]	$1.35e^{5}$	$1.35e^{5}$	$1.40e^{5}$	$2.74e^{5}$

Table 2 Arrhenius Parameter [19] [30]

3.5 Electrochemical–Thermal Coupling

The coupling between the electrochemical model and the thermal model is a key aspect in the numerical simulation of lithium-ion batteries,

particularly when studying safety-related phenomena such as thermal runaway. In electro-thermal models, the two domains are strongly interconnected through several nonlinear relationships, which arise from the dependence of electrochemical processes on temperature and, conversely, from the generation of heat during battery operation. This bidirectional interaction leads to a system of highly nonlinear equations that must be solved simultaneously. One of the main nonlinearities arises from the temperature dependence of reaction kinetics, typically described through Arrhenius-type relations, in which the exchange current density and reaction rate constants increase exponentially with temperature. A second important source of nonlinearity is associated with the Butler–Volmer equation, which relates the interfacial current density to the overpotential in an exponential manner and is itself affected by temperature-dependent kinetic parameters. Additional nonlinearities arise from the temperature dependence of transport properties, such as lithium diffusion coefficients in the solid particles and electrolyte, ionic conductivity, and electrolyte diffusivity, all of which typically follow Arrhenius-type expressions. The electrochemical model also contributes to heat generation through several mechanisms, including ohmic (Joule) heating, reaction heat, and entropic heat, each of which depends on the local current density, overpotential, and state of charge, further strengthening the coupling between electrochemistry and temperature.

When specifically focusing on thermal runaway modeling, not all nonlinear couplings play the same role. The most critical mechanisms are those responsible for the positive feedback between temperature rise and heat generation. In particular, the Arrhenius dependence of reaction kinetics is essential, as it leads to a rapid increase in reaction rates as temperature rises, which in turn produces additional heat. Similarly, the

Butler–Volmer kinetics, combined with temperature-dependent exchange current density, contributes to the amplification of heat generation under high current or short-circuit conditions. Another crucial element is the inclusion of exothermic side reactions, such as SEI decomposition, electrolyte reduction, and cathode decomposition, whose reaction rates also follow Arrhenius-type kinetics and can release large amounts of heat once a critical temperature is reached. These mechanisms form the core feedback loop responsible for thermal runaway. Other temperature-dependent transport properties, while important for accurately describing battery performance, generally play a secondary role in triggering runaway conditions. Therefore, in thermal runaway models, the most essential nonlinear couplings are those linking temperature, reaction kinetics, and heat generation, as they determine the self-accelerating behavior that characterizes the onset of thermal instability in lithium-ion cells.

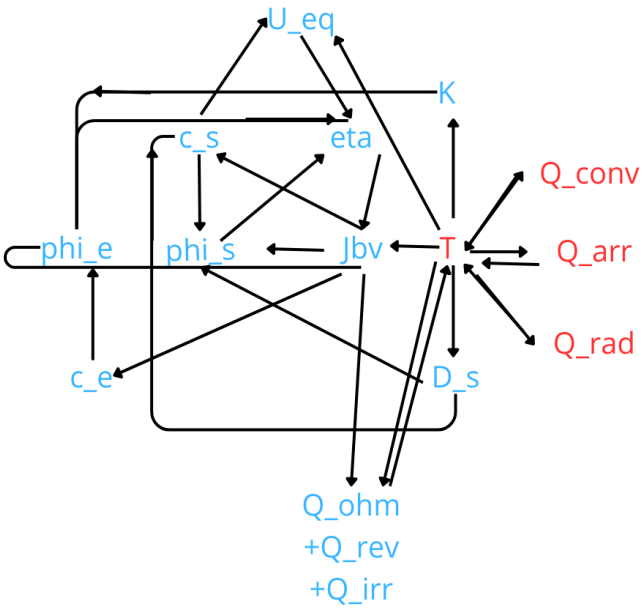

Figure 11 Non linear coupling of system: in blue the variable of electrochemical model, in red the variable of thermal model

3.6 Model Assumptions and Limitations

The electro-thermal model adopted in this work relies on several simplifying assumptions that allow the main physical processes governing lithium-ion battery operation to be captured while maintaining a manageable computational cost. First, the cell is described using a pseudo-two-dimensional (P2D) electrochemical formulation, in which lithium transport in the electrolyte is modeled along the through-thickness direction of the electrodes, while lithium diffusion within the active material particles is assumed to occur only in the radial direction. The complex porous microstructure of the electrodes is therefore not explicitly resolved but instead represented through homogenized effective properties, such as effective ionic conductivity, electronic conductivity, and diffusion coefficients. From a thermal perspective, the model assumes that the thermophysical properties of the materials—such as density, heat capacity, and thermal conductivity—are uniform within each domain, and that heat transfer occurs mainly through conduction inside the cell, while convective and radiative heat fluxes are applied at the external boundaries. Heat generation is calculated from the electrochemical model by accounting for contributions such as ohmic heating, reaction heat, and entropic heat, while the kinetics of electrochemical and side reactions are described through Arrhenius-type temperature dependencies. Additionally, the model assumes local thermal equilibrium between the different phases of the porous electrodes and neglects possible geometric changes of the cell during operation.

Despite these simplifications, the model presents some limitations. The homogenized P2D approach does not explicitly capture the detailed microstructural heterogeneity of the porous electrodes, which may lead to local variations in current density and temperature that are not fully resolved at the macroscopic scale. Furthermore, the model does not include mechanical deformation or structural failure mechanisms, such as separator rupture, electrode fracture, or particle cracking, which may play a role in the initiation of internal short circuits under severe abuse conditions. The kinetics of exothermic side reactions are also represented using simplified Arrhenius expressions based on experimentally derived parameters, which may not fully reproduce the complexity of the chemical degradation pathways occurring during extreme thermal events. Nevertheless, the model retains the key electro-thermal coupling mechanisms responsible for the positive feedback between temperature rise and heat generation. For this reason, despite its simplifying assumptions, the adopted framework provides a physically consistent and computationally efficient tool for investigating the conditions leading to thermal runaway and for analyzing the thermal stability of lithium-ion cells.

4. Implementation of the Model in COMSOL Multiphysics

4.1 Description of the COMSOL Environment

COMSOL Multiphysics is a finite element–based simulation environment widely used for the modeling and analysis of complex physical systems involving multiple interacting phenomena. One of the main strengths of COMSOL lies in its ability to solve coupled multiphysics problems within

a unified framework, allowing different physical domains such as electrochemistry, heat transfer, fluid dynamics, and structural mechanics to be simultaneously considered. The software provides a flexible interface in which the governing equations of each physical process can be implemented through dedicated physics modules or defined directly by the user when more customized formulations are required. In addition, COMSOL allows the definition of material properties, boundary conditions, and source terms in a highly modular way, which facilitates the construction of models that accurately represent real physical systems. The numerical solution is obtained through the finite element method, which discretizes the computational domain into smaller elements and solves the governing equations over this mesh. This approach enables the accurate resolution of spatial variations of the modeled variables, even in the presence of strong gradients or nonlinear couplings between different physical fields. Thanks to these capabilities, COMSOL has become a widely adopted tool in both academic research and industrial applications for the simulation of multiphysics systems, including electrochemical devices such as lithium-ion batteries.

In this work, COMSOL Multiphysics is used to implement a coupled electrochemical thermal model of a lithium-ion battery in order to investigate the mechanisms leading to thermal instability and, potentially, thermal runaway. The model combines the electrochemical description of the cell with a heat transfer formulation, allowing the interaction between electrical, chemical, and thermal phenomena to be captured within the same computational framework.

Within COMSOL, these interactions are implemented through user-defined variables and non-local couplings, which allow the governing equations of the different physical processes to be solved simultaneously.

This integrated approach makes it possible to analyze how electrochemical operation influences temperature evolution and, conversely, how temperature variations affect the internal processes of the battery.

4.1.1 Mesh in Comsol

The electrochemical variables were discretized along a one-dimensional domain representing the thickness of the cell, including the electrodes and separator. A structured mesh was adopted using a distribution-based approach, allowing full control over the number and spacing of elements in each region. This is particularly important in lithium-ion battery models, where steep gradients of potential and concentration can arise, especially under high-current conditions such as internal short circuits. The mesh parameters were selected to ensure sufficient resolution of these gradients while maintaining numerical stability and computational efficiency. A moderate growth rate was used to provide a smooth transition between elements of different sizes, avoiding abrupt changes that could affect convergence. This discretization enables an accurate representation of the electrochemical behavior of the cell.

The pseudo-dimensional domain used to describe solid-phase diffusion in the electrodes was discretized using a structured mapped mesh. In this representation, two separate rectangular domains were defined to model the cathode and anode, respectively. Each domain accounts for the coupling between the spatial coordinate along the electrode thickness and the radial coordinate within the active material particles, resulting in a pseudo-two-dimensional formulation. The mesh was constructed with a regular distribution of quadrilateral elements, ensuring numerical stability

and accuracy in the solution of the diffusion equation in the solid phase. This approach allows capturing the concentration gradients both across the electrode and within the particles.

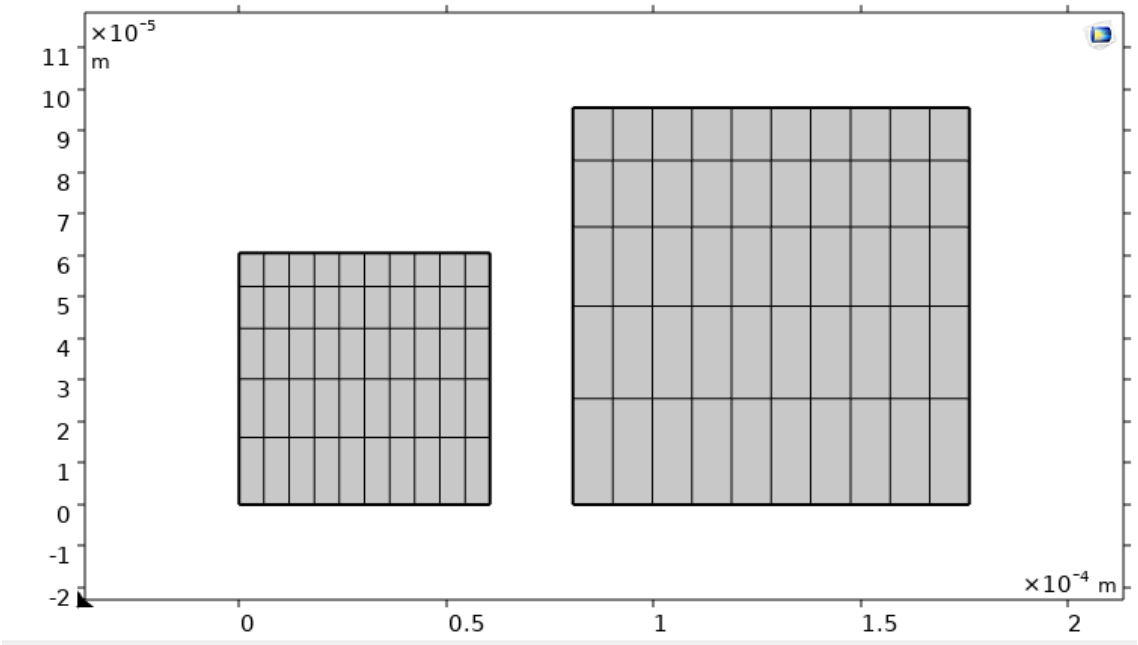

Figure 12 Mesh of Pseudo Dimension

It is worth noting that the mesh adopted for the thermal domain appears significantly finer compared to the electrochemical discretization. This is mainly due to the physics-controlled meshing strategy implemented in COMSOL, which automatically refines the mesh in the presence of strong nonlinearities and coupled source terms. In particular, the inclusion of multiple heat generation mechanisms, such as ohmic and Arrhenius-based contributions, introduces steep temperature gradients during the thermal runaway process. As a result, a finer discretization is required to accurately resolve these variations and ensure numerical stability. Moreover, the two-dimensional nature of the thermal model further increases the number of elements, as the temperature field must be resolved in both spatial directions. Therefore, the higher mesh density is

consistent with the complexity of the thermal problem and contributes to improving the accuracy of the simulation results.

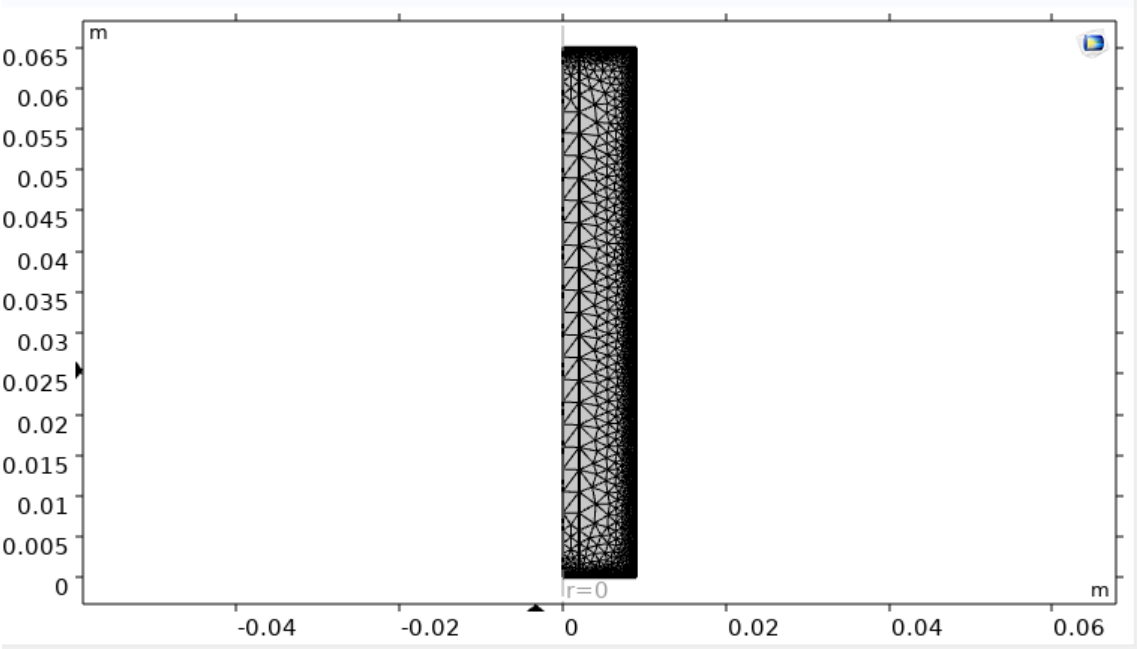

Figure 13 Mesh for Thermal model

4.2 Physics and Mathematics Implemented

4.2.1 Electrochemical Model in Comsol

In this work, different approaches are adopted to implement the equation listed in chapter 3. For the electrochemical model, PDE (partial differential equations) in the general form are used to have control of every single element of the equation.
PDEs express how a physical quantity, such as concentration, or electric potential, varies in space and time as a result of transport processes, source terms, and interactions with other fields. Within the COMSOL environment, these equations are typically implemented through dedicated physics interfaces, where the software automatically formulates the underlying PDEs based on the selected physical model and the specified material properties and boundary conditions.

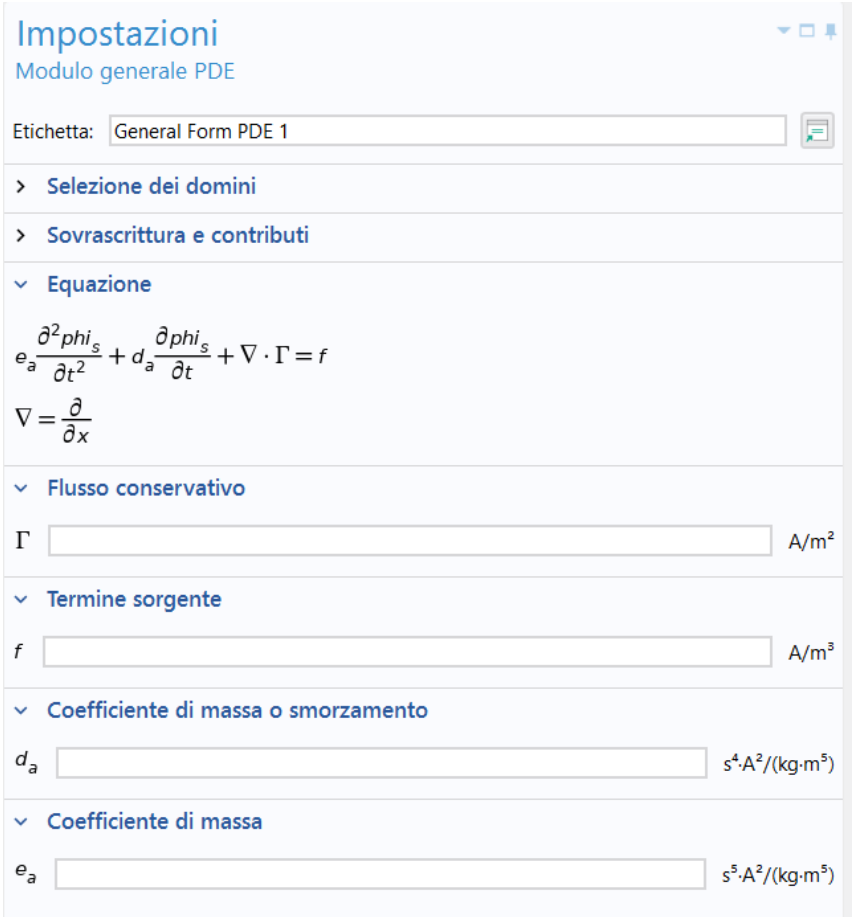

Figure 14 PDE interface in comsol

In particular, in the electrochemical model PDEs are used for the equation (1) - Law of conservation of mass in solid body-, (2) - Law of conservation of mass in electrolyte-, (3) - Law of conservation of charge in the solid phase-, (4) -Law of conservation of charge in electrolyte-.

Another method used in this work is the ODE interface; COMSOL Multiphysics also allows the implementation of ordinary differential equations that are not associated with spatial variables through the Global ODEs and DAEs interface. These equations are typically used to describe the time evolution of variables that depend only on time and not on spatial coordinates. Within the modeling framework, global ODEs are particularly useful for representing lumped processes, global balances, or reaction kinetics that affect the entire system rather than a specific spatial domain. The equations are solved simultaneously with the other governing equations of the model and can be directly coupled with the variables defined in the different physics interfaces. This makes it possible to include additional dynamic processes in the simulation, such as time-dependent reaction rates, degradation mechanisms, or global source terms that interact with the multiphysics model. By integrating these equations into the overall numerical system, COMSOL ensures that the evolution of the global variables remains fully consistent with the spatially distributed fields described by the partial differential equations.

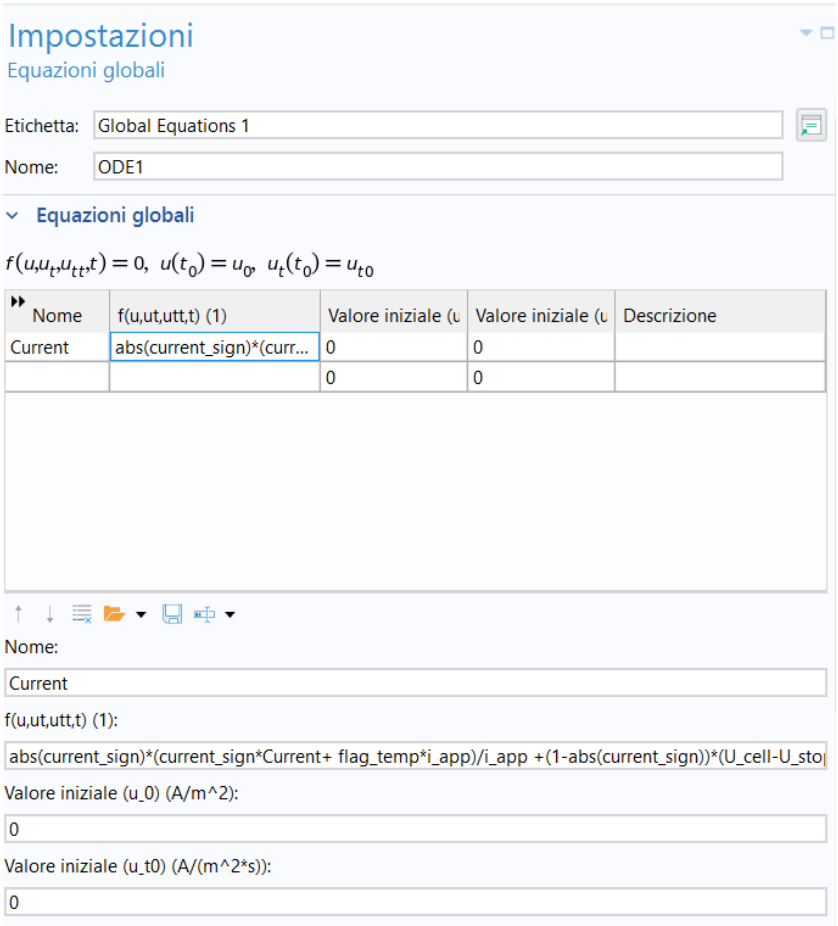

Figure 15 ODE interface in comsol

In this work, ODEs are used as Mikail shows in his thesis [12] to write an equation for the charging current imposed at the positive electrode, defined as follow:

$$abs(current_{sign})\frac{current_{sign} * current + flag_{temp} * i_{app}}{i_{app}} + \left(1 - abs(current_{sign})\right)\frac{U_{cell} - U_{stop}}{U_{stop}} = 0$$

Where Current is the name of the variable, i_{app} is the 1C charging current, U_{cell}, U_{stop} are respectively the current voltage and maximum voltage of the cell. $current_{sign}$ and $flag_{temp}$ are two indicators that change their value according to events. Varying these two, different charging modes can be realized: it possible to charge the battery with a current at full scale, charging it to the maximum SOC after the maximum voltage is reached, discharge the battery simulating a load and leave the battery in a 'stationary state'.

Charging mode	Current sign	Flag temp
DC charging	1	1
DC discharge	-1	1
Constant voltage charge	0	0
Relaxation	1	0

Table 3 Values of indicators [12]

In COMSOL Multiphysics, the Events interface is used to introduce discrete changes in the simulation when specific conditions are met during the time-dependent solution. Unlike the continuous behavior described by partial differential equations or ordinary differential equations, events allow the model to account for situations in which certain variables or parameters must be modified abruptly at a given time or when a predefined threshold is reached. This functionality is particularly useful when modeling systems that exhibit switching behaviors, control actions, or sudden changes in operating conditions. Events can be triggered either at predetermined times or when a user-defined condition involving one or more model variables becomes true. Once the event is activated, COMSOL can update selected variables, parameters, or equations before continuing the time integration of the

model. In this way, the Events interface provides a flexible tool for representing discontinuous processes within a time-dependent multiphysics simulation while maintaining consistency with the underlying numerical solution.

In this model, the indicators change value when a maximum/minimum SOC is reached or when the maximum voltage of the cell is reached.

4.2.2 Thermal Model in Comsol

In this work, the thermal problem is implemented in COMSOL Multiphysics using the *Heat Transfer in Solids* physics interface. This interface provides a predefined framework for solving heat transfer problems within solid domains and allows the user to easily define the different contributions involved in the thermal balance through dedicated nodes in the model tree. Within this environment, the temperature field is treated as the main dependent variable and is computed over the entire computational domain during the time-dependent simulation. The interface also allows additional physical contributions to be included in a modular way by adding specific sub-nodes that represent different thermal effects. In the present model, the heat generated inside the battery is introduced through a volumetric heat generation node, which accounts for the internal heat sources calculated from the electrochemical model. In addition, boundary nodes are used to represent the heat exchange with the external environment. In particular, convective heat flux and surface-to-ambient radiation nodes are included to model the heat dissipated from the outer surface of the cell. This node-based structure of the COMSOL interface makes it possible to clearly organize the different thermal

contributions within the model and to easily couple them with the variables computed in the other physics interfaces.

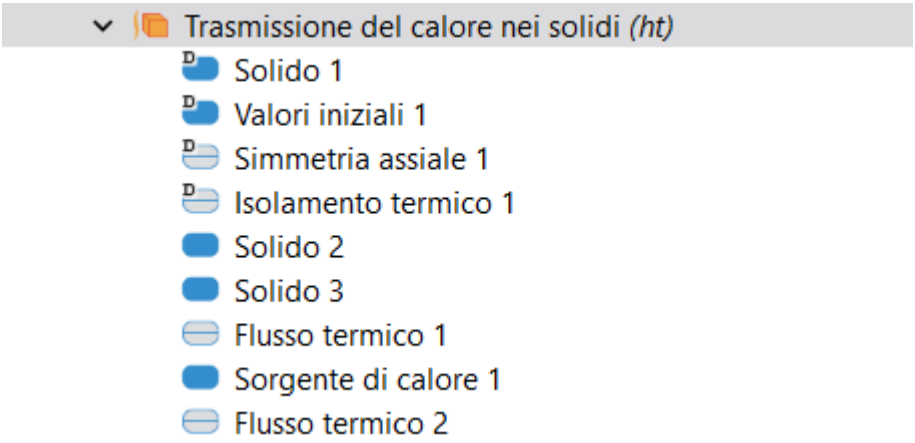

Figure 16 Thermal nodes-structure

The Arrhenius equation in the thermal model are defined with the PDEs already described.

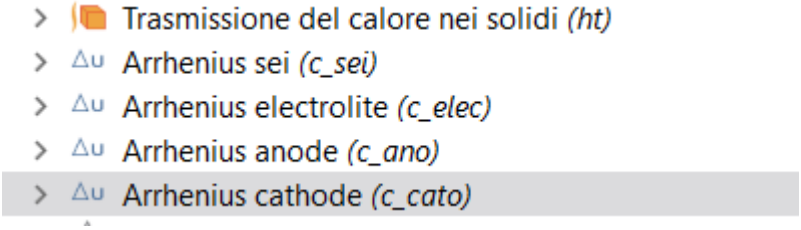

Figure 17 Thermal Model in comsol

4.3 Coupled Physics Setup

1) Electrochemical component 1d ←→Pseudo dimension component

In the model developed in this work, the coupling between the two electrochemical components namely the one-dimensional domain

representing the cell thickness and the additional pseudo dimension used to describe lithium diffusion within the active material particles is implemented in COMSOL through the use of nonlocal coupling operators. In particular, the *Linear Extrusion* operator is employed to map variables between the different geometric domains. This operator allows quantities defined in one domain to be evaluated and used in another domain, even when the two domains do not share the same spatial coordinates. In the present case, the electrochemical variables calculated along the one-dimensional electrode domain, such as electrolyte concentration and potentials, must be linked to the pseudo-dimensional domain where solid-state diffusion within the electrode particles is described. The linear extrusion operator provides a convenient way to transfer these quantities between the two components by establishing a direct correspondence between their spatial coordinates. In this way, the variables defined in the main 1D electrochemical model can be consistently used within the equations governing the pseudo dimension, ensuring that the coupled electrochemical processes are solved in a coherent and integrated manner within the COMSOL framework.

The nonlocal coupling is defined calling the linear extrusion operator inside the 1d component to map the butler Volmer current in the pseudo dimension, and calling the linear extrusion operator inside the pseudo dimension to map the solid concentration in the 1d dimension.

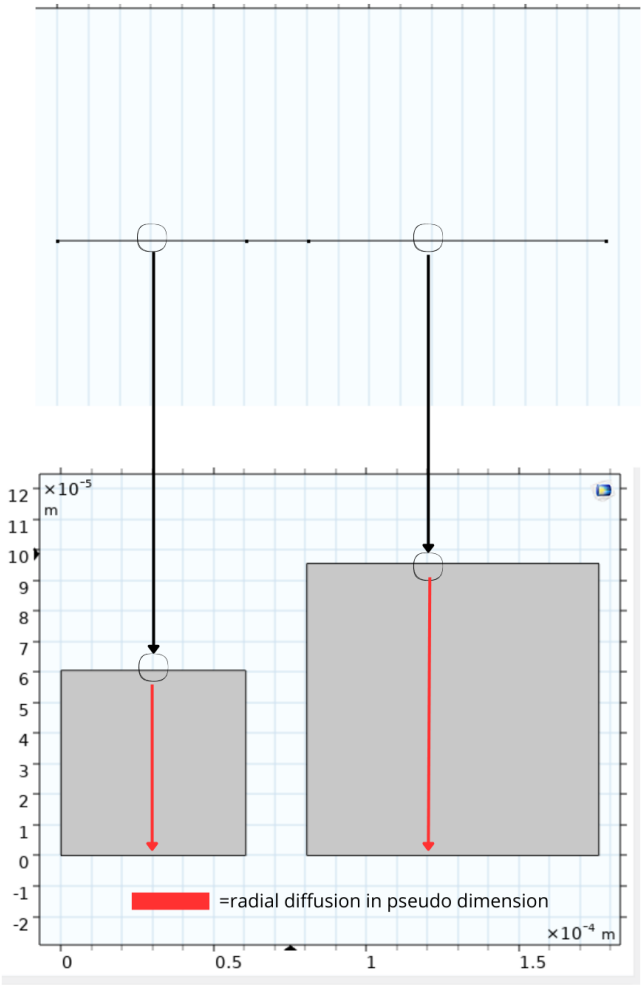

Figure 18 1d-pseudo-space coupling

2) Electrochemical components ←→Thermal components

The coupling between the electrochemical model and the thermal model is implemented in COMSOL through the use of a nonlocal coupling operator, specifically the *Average* operator (aveop). Since the electrochemical model and the thermal model are defined on different computational components and in the thermal model are not defined anode, cathode and electrolyte, a direct pointwise coupling between their variables is not possible. The average operator is therefore used to transfer information between the two domains by computing the spatial average

of selected electrochemical quantities and making them available to the thermal model. In particular, the heat generation terms calculated in the electrochemical component are averaged over the electrochemical domain and then introduced as volumetric heat sources in the thermal model. The use of averaged quantities is justified by the fact that the thermal model describes the macroscopic temperature distribution of the cell, while the electrochemical variables are defined at a smaller spatial scale. Therefore, representing the electrochemical contributions through their spatial average allows the thermal model to capture the overall heat generation within the cell without introducing unnecessary spatial complexity. This approach provides a consistent and computationally efficient way to couple the two physics while preserving the main electro-thermal interactions governing the system behavior.

In the implementation of the electro-thermal model, the nojac operator available in comsol is used to improve the numerical stability and efficiency of the simulation. The nojac command allows a variable or expression to be evaluated without including its contribution in the Jacobian matrix during the nonlinear solution process. In practice, this means that the selected expression is treated as an explicit quantity during the iteration, avoiding additional couplings that would otherwise increase the complexity of the system of equations. In the present model, this operator is used in two specific situations. First, it is applied when the temperature computed in the thermal component is accessed within the electrochemical model, preventing the solver from unnecessarily expanding the Jacobian with additional cross-dependencies between the two components. Second, the nojac operator is used in the Arrhenius expressions describing the temperature dependence of the reaction rates,

where the temperature appears inside exponential terms. In these cases, excluding the Arrhenius expressions from the Jacobian helps reduce numerical stiffness and facilitates convergence of the nonlinear solver. Overall, the use of the nojac operator allows the electrochemical and thermal models to remain consistently coupled while maintaining a more stable and computationally efficient solution process.

4.4 Initial Conditions

In time-dependent multiphysics simulations, the definition of appropriate initial conditions plays an important role in ensuring both the physical consistency of the model and the stability of the numerical solution. Initial conditions define the starting values of the dependent variables such as temperature, concentrations, and electric potentials at the beginning of the simulation and therefore determine the state from which the solver begins the time integration. If these values are not chosen consistently with the physical behavior of the system, the solver may encounter large initial residuals or nonphysical gradients, which can negatively affect convergence and increase the computational cost of the simulation. In strongly coupled and nonlinear models, such as electro-thermal battery simulations, this aspect becomes even more critical because the different physical variables are closely interconnected. In COMSOL, carefully defining the initial conditions helps the nonlinear solver start from a physically reasonable state, reducing the number of iterations required at the first time step and improving the overall robustness of the solution process. For this reason, initial values are typically selected to represent a realistic operating condition of the system, allowing the solver to progressively evolve the solution in time without introducing unnecessary numerical instabilities.

In this model initial condition are imposed for the main variable described firstly; the values of the initial conditions of course change with respect to the situation that the model wants describe (could be a charging mode, discharge or stationary state at a determined SOC)

4.5 Implementation of Thermal Runaway Mechanisms

In this work, particular attention is given to internal short circuits caused by nail penetration, as the available experimental data used for validation were obtained from tests performed under these conditions. Nail penetration is a commonly used abuse test to intentionally trigger internal short circuits and study the resulting electrochemical and thermal response of lithium-ion cells. For this reason, the modeling approach developed in this study focuses on reproducing the effects associated with this type of mechanical damage. Nevertheless, the implemented framework is sufficiently flexible to be adapted to other types of internal short circuits. By appropriately modifying the parameters governing the conductive pathway or the triggering conditions, the model can also be used to represent electrically or thermally induced short circuits, allowing the same formulation to be extended to different thermal runaway scenarios.

In the present model, the internal short circuit is implemented by introducing an electronic conductivity in the separator region [21], which allows current to flow directly between the negative and positive electrodes. Within the framework of the electrochemical model, this is achieved by assigning a finite value of electronic conductivity to the separator, which is normally assumed to be electrically insulating. Since

the model adopts a one-dimensional geometry along the cell thickness, this approach effectively represents a short circuit distributed over the entire electrode area. However, real internal short circuits typically occurs over a localized region of the cell. In order to account for this limitation and avoid unrealistically high short-circuit currents, the conductivity assigned to the separator is reduced, representing an effective conductive pathway corresponding to a localized defect within the cell. This approach allows the short-circuit current to arise naturally from the charge conservation equations of the electrochemical model. In contrast to other modeling approaches found in the literature [6] [20] [22] where the internal short circuit is introduced through an external equivalent resistance connected to the electrical circuit, the present formulation incorporates the short circuit directly within the electrochemical domain. As a result, the current distribution and the associated heat generation remain consistent with the underlying electrochemical physics of the system.

In order to represent the onset and duration of the internal short circuit, the electronic conductivity of the separator is defined through a time-dependent expression. In particular, the separator conductivity is written as

$$\sigma_{sep} + (\sigma_{sep,sc} - \sigma_{sep})\, flc2hs(t - t_{start}, \tau)\, flc2hs(t_{end} - t, \tau).$$

In this formulation, σ_{sep}represents the nominal electronic conductivity of the separator under normal operating conditions, while $\sigma_{sep,sc}$corresponds to the effective conductivity associated with the short-circuit state. The two smoothed Heaviside functions $flc2hs(\cdot)$, available

in COMSOL, are used to activate the short circuit within a specific time interval. The first function gradually switches the conductivity from its nominal value to the short-circuit value at the time t_{start}, while the second function ensures that the increased conductivity is maintained only until t_{end}. The parameter τcontrols the smoothness of the transition, avoiding abrupt discontinuities that could lead to numerical instabilities in the solver. In this way, the short circuit is introduced in a controlled and numerically stable manner, allowing the model to reproduce the temporal evolution of the short-circuit event.

The duration of the internal short circuit ($t_{end} - t_{start}$)is selected such that the simulation captures the electrochemical processes that dominate the initial phase of the event. During the short circuit, very large currents develop, leading to strong concentration gradients within the electrolyte. As the event progresses, ionic diffusion becomes the limiting process, and the local availability of lithium ions may approach depletion conditions. Under these circumstances, the electrochemical operation of the cell is no longer sustainable, and the system's behavior progressively shifts toward a regime dominated by ohmic currents and heat generation. For this reason, the duration of the imposed short circuit is chosen so that the model describes the electrochemically controlled phase of the event, while the subsequent evolution is mainly governed by thermal processes and material decomposition reactions associated with thermal runaway.

4.6 Numerical Solution Strategy

The numerical solution of the coupled electrochemical–thermal model is obtained in COMSOL using a time-dependent solver, which allows the temporal evolution of the system variables to be computed while

accounting for the interactions between the different physical processes. The governing equations of the model, including both partial differential equations and ordinary differential equations, are discretized in space using the finite element method, while the time integration is performed through an implicit time-stepping scheme. This approach is particularly well suited for multiphysics problems characterized by strong nonlinearities and potentially stiff equations, as it provides improved numerical stability during the transient simulation. During the solution process, the discretized equations form a nonlinear algebraic system that is solved iteratively at each time step using a Newton-based method.

In order to handle the strong coupling between the electrochemical and thermal variables, the model is solved using a fully coupled solver approach. In this formulation, all the dependent variables of the system are solved simultaneously within a single nonlinear system. This strategy is particularly advantageous in the present case because the electrochemical and thermal models are tightly interconnected through several bidirectional dependencies, such as the influence of temperature on transport properties and reaction kinetics, and the contribution of electrochemical processes to heat generation. An alternative strategy available in COMSOL is the segregated approach, where the variables are solved in separate groups in an iterative sequence. While this method can reduce memory requirements for some problems, it may struggle to converge when the physical couplings between variables are strong. For this reason, the fully coupled approach is preferred in this model, as it provides a more robust and stable solution when dealing with the highly nonlinear electro-thermal interactions that characterize lithium-ion battery simulations, particularly under conditions that may lead to thermal runaway.

5. Experimental Campaign

5.1 Objectives of the Experimental Tests

The experimental campaign was conducted with the main objective of investigating the safety behavior of the lithium-ion cell under severe abuse conditions and of providing reliable data for the validation of the electrochemical–thermal model developed in this work. In particular, the tests aim to reproduce an internal short circuit generated by mechanical damage, which represents one of the most critical failure mechanisms leading to thermal runaway in lithium-ion batteries. By performing controlled mechanical abuse experiments, it is possible to monitor the thermal response of the cell during the short-circuit event and the subsequent evolution of the system. The measurements obtained from these tests, such as temperature profiles, provide valuable information on the onset of self-heating phenomena and on the progression of the failure process. These experimental results are therefore used both to improve the understanding of the mechanisms governing thermal runaway and to support the calibration and validation of the numerical model developed in this study.

Among different experimental techniques available, calorimetric methods are widely used to study the thermal stability of cells and the mechanisms leading to thermal runaway. In particular, the Accelerating Rate Calorimeter (ARC) is commonly employed to monitor the self-heating behavior of batteries under controlled conditions. This instrument allows the detection of exothermic reactions and provides detailed information on the temperature evolution of the cell during failure events. The use of ARC systems for the investigation of lithium-ion battery safety has been widely reported in the literature, where they have been applied to

characterize the onset of thermal runaway and the associated heat generation processes [23] [24] [25].

5.2 Description of the Tested Cells

During the experimental tests three different cylindrical cells are used:

JGNE JGPFR18650 3,2V (1100 mAh)
SAMSUNG INR21700-50E (4900 mAh)
SAMSUNG INR18650-35E 3,6V (3400 mAh)

In particular the results achieved with the model are compared with the Samsung of 3400 mAh. In the table below the main characteristics are listed.

Parameters	**information**
Technology	LiNiMnCo
Nominal Capacity	3400 mAh
Nominal Voltage	3.6
Charging Voltage	4.2
Charging Current	0.5C (1,700mA)
Operating Temperature Range	Charge : 0 to 45°C (Ambient) Discharge : -20 to 60°C (Ambient)
Weight	50 g
Geometry	Height : Max. 65.25 mm Diameter: Max. Φ 18.50 mm

Table 4 Properties of the tested cell

5.3 Instrumentation and Data Acquisition

To carry the experiments two instruments are used: THT ARC and a Testo probe.

The THT ARC system is composed of two components that allow the safe execution and monitoring of abuse tests on lithium-ion cells.

a) Inner chamber. The internal chamber hosts the cell during the experiment and includes a dedicated support system to properly position the battery. This chamber also contains the mechanical actuator used to drive the nail during nail penetration tests. The chamber walls are equipped with a heating system that can raise the ambient temperature inside the enclosure, allowing tests to be performed at temperatures higher than room temperature or enabling overheating experiments. Several thermocouples are installed inside the chamber, including one that is directly attached to the surface of the cell in order to monitor its temperature during the test. The chamber is also equipped with an exhaust outlet to allow the release of gases and fumes generated during abuse conditions. Additionally, an inspection window and a thermal imaging camera are integrated into the chamber to visually monitor the thermal reactions occurring during the experiment.

b) Outer chamber. The external enclosure surrounds the inner chamber and acts as a secondary containment system for the gases and fumes produced during the test. These emissions are extracted through a dedicated ventilation system, filtered, and then safely released to the atmosphere. This outer compartment also houses additional instrumentation used for different experimental configurations.

c) Control system and power electronics. The THT ARC setup includes a power electronics unit that manages the various sensors and devices installed in the system. The data collected from these components are transmitted to a computer and visualized through the software THT Abuse, which serves as the main user interface for controlling the instrument and recording experimental data. The software also allows the user to configure different testing procedures and to store the collected information for subsequent analysis.

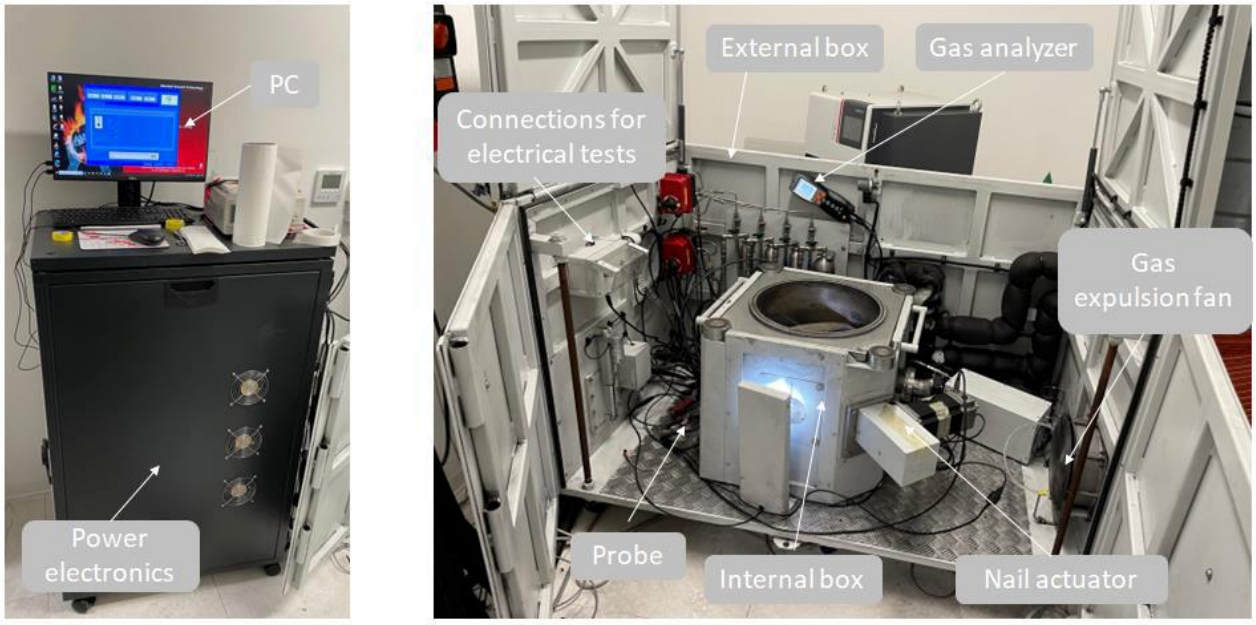

Figure 19 THT ARC components

A Testo 330 probe permits to monitor the composition of the gases generated during the thermal runaway event of the cell. This instrument allows the measurement of several gaseous species typically produced during battery failure, including carbon monoxide (CO), nitric oxide (NO), and oxygen (O_2), which are specifically analyzed in the present experimental study. The sensing probe of the analyzer was positioned at the gas outlet of the inner chamber of the THT ARC system, allowing the sampling of the fumes released during the experiment and enabling the characterization of the gas emissions associated with the abuse event.

Figure 20 Testo Probe

5.4 Experimental Results

For the SAMSUNG INR18650-35E 3,6V three tests are conducted and the results are reported in the graph below.

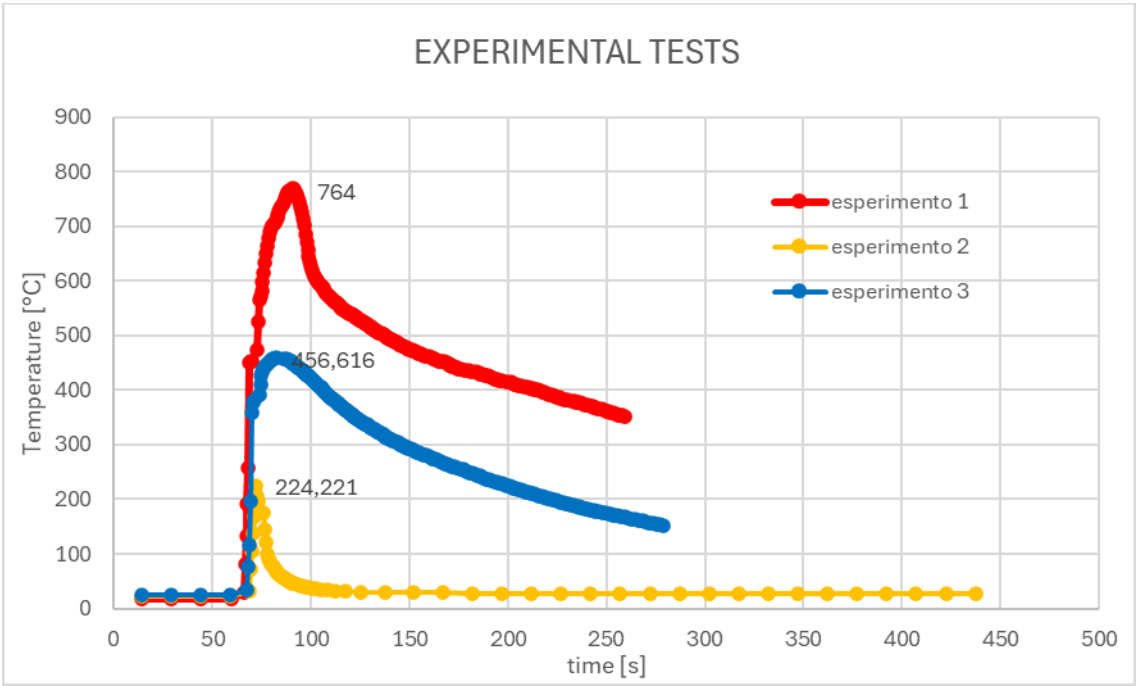

Figure 21 Experimental tests

The analysis of the experimental results highlights a qualitatively consistent behavior among the different tests performed. As shown in Figure 21, the curves corresponding to the two experiments considered exhibit a similar

temporal evolution: the signal initially remains close to zero, followed by a rapid growth phase leading to the occurrence of a peak, and finally by a progressive decay phase. Despite the good reproducibility of the overall trend of the phenomenon, significant differences can be observed in the maximum values reached in the two tests, with one experiment characterized by a noticeably higher peak than the other. This variability can be attributed to unavoidable differences in the experimental conditions and to the intrinsically complex and sensitive nature of the thermal runaway phenomenon. Moreover, the variability can depend also on the chosen position of the thermal probe, a different chemical composition of the tested cells (the producers often declare a variable composition [30]) and possible difference in the SOC.

It can also be observed that, in the experiment characterized by the higher peak value, the initial decay phase is faster compared to the other test. This behavior can be associated with the stronger contribution of heat dissipation mechanisms at higher temperatures, in particular radiative heat transfer, whose intensity rapidly increases with temperature according to the Stefan–Boltzmann law. As a consequence, the higher temperatures reached during the peak lead to a stronger initial energy dissipation and therefore to a faster reduction of the signal immediately after the maximum value is reached.

A further difference concerns the temporal position of the peak, which occurs slightly later in the experiment characterized by the higher maximum value. This behavior can be explained by considering that, when a larger amount of energy is released, the system continues to accumulate heat for a longer period before the dissipative mechanisms become dominant. As a result, the signal continues to increase for a slightly longer time, leading to a delayed occurrence of the peak.

Finally, a third experiment, initially carried out under the same operating conditions, was not considered in the model validation analysis because it exhibited significantly lower values compared to the other tests. This behavior suggests that the short circuit triggered during that test did not generate a sufficiently intense heating to fully activate the exothermic reactions described by the Arrhenius kinetics. Consequently, the observed

phenomenon cannot be considered representative of the thermal runaway dynamics investigated in the present work, and the corresponding dataset was excluded from the comparison with the other experimental results.

Figure 22 The two cells after the test

In the observed experimental results, carbon monoxide (CO) is released in significant quantities only after the cell temperature peak has been reached. This behavior can be explained by considering the nature of the reactions contributing to thermal runaway. The initial thermal peak is primarily generated by the fastest exothermic reactions—such as the decomposition of the SEI layer, the anode-electrolyte interaction, and the partial decomposition of the cathode—which releases heat before the decomposition of the electrolyte's organic solvents can fully develop. Indeed, CO production is mainly linked to these latter reactions, which require higher temperatures and are thus activated only during the advanced stages of the runaway reaction.

Furthermore, the gas produced inside the cell is not immediately released into the external environment: the internal pressure must build up until it triggers the opening of the exhaust channels or the vent hole, introducing a further delay between CO formation and its detection by the probe. The time required for the gas to reach the probe also contributes to this lag. Therefore, the delayed appearance of carbon monoxide in the measured profile does not indicate an absence of initial production, but rather reflects both the sequence

of exothermic reactions within the cell and the dynamics of gas accumulation and release.

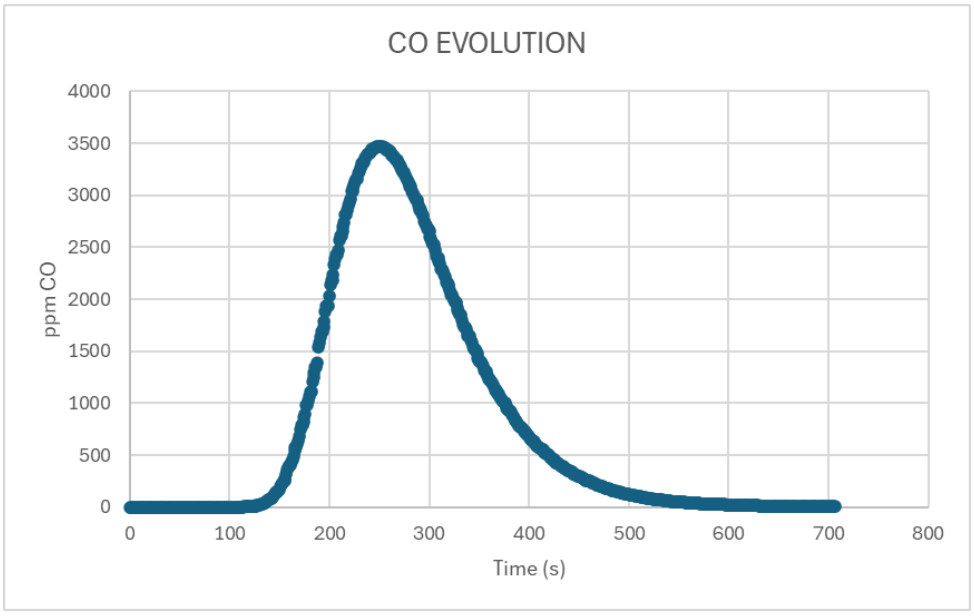

Figure 23 CO Evolution in time

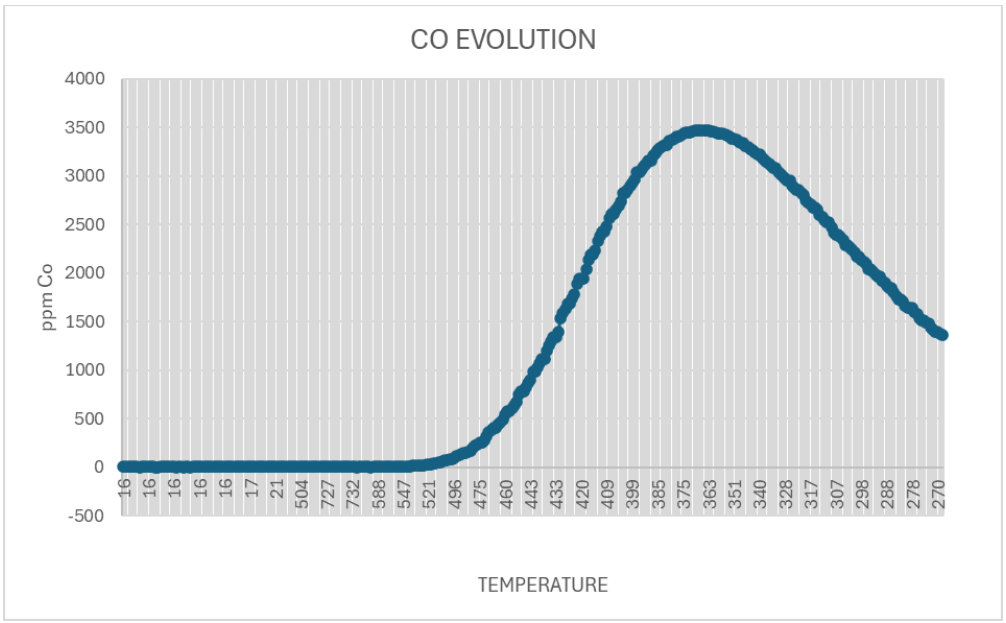

Figure 24 CO Evolution with Temperature

6. Results and Model Validation

This section presents the main results obtained from the numerical simulations and their comparison with the experimental data. First, the outcomes of the electrochemical–thermal model are illustrated, highlighting the key features of the cell response under internal short-circuit conditions. Particular attention is given to the evolution of temperature and other relevant variables that characterize the onset and progression of the failure event. Subsequently, the numerical results are compared with the data obtained from the experimental campaign, in order to assess the accuracy and reliability of the model. This comparison allows the validation of the modeling approach by evaluating its capability to reproduce the main trends observed during the experiments.

6.1 Model Results

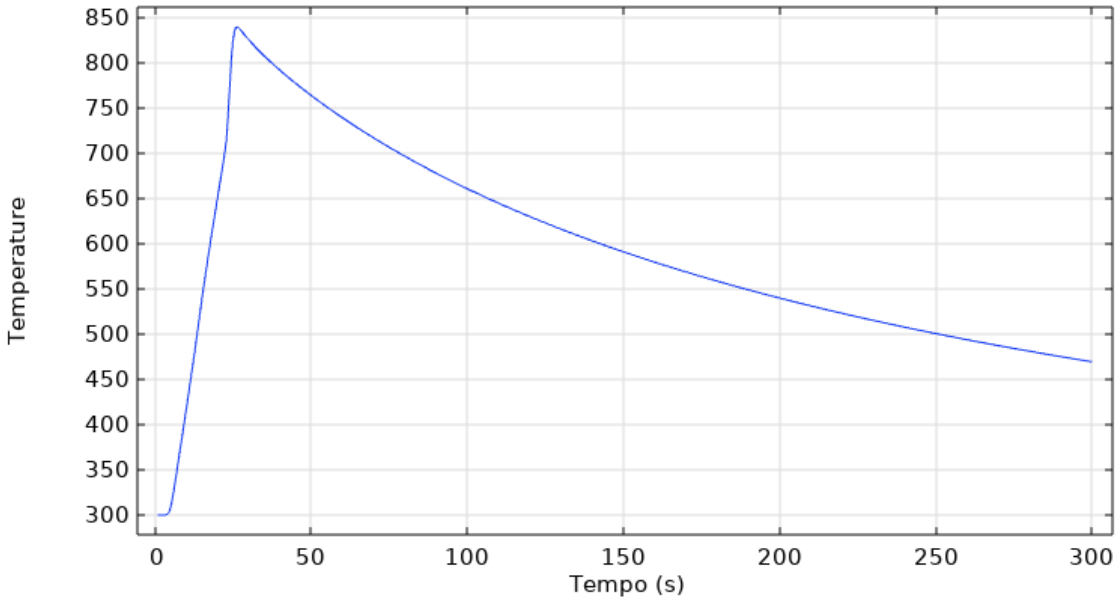

Figure 25 Temperature [K] Profile of the Model

The temperature profile predicted by the model shows a characteristic evolution that is consistent with the expected behavior of a lithium-ion cell undergoing an internal short-circuit event. Starting from an initial value

close to ambient conditions (around 300 K), the temperature rapidly increases within a short time interval, reaching a peak of approximately 830–840 K. This sharp rise is associated with the sudden onset of intense heat generation, primarily driven by the short circuit and the activation of exothermic processes within the cell. Following this peak, the temperature gradually decreases over time, indicating that heat dissipation mechanisms such as conduction and external losses begin to dominate once the main heat sources are reduced or exhausted. Overall, this behavior reflects the ability of the model to capture both the rapid escalation phase and the subsequent relaxation phase, which are key features of thermal runaway phenomena.

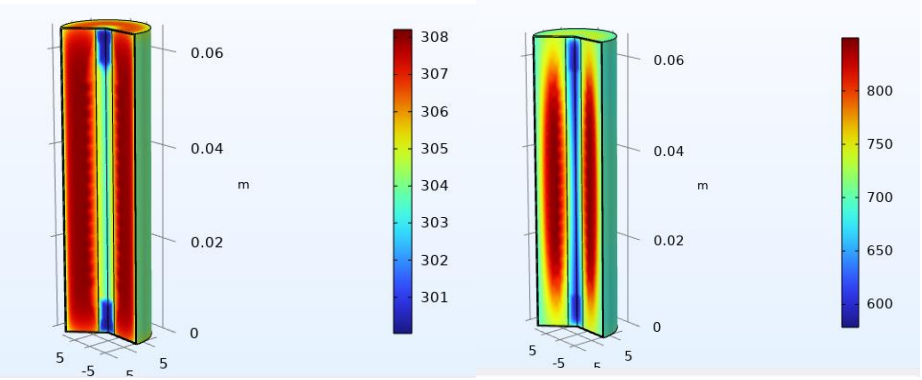

Figure 26 3d Temperature for the instant of sc, and for the instant where max T is reached

It is possible to notice that when the maximum temperature is reached the distribution inside the cell is not homogeneous, this behavior is due to the strong gradient given by the activation of electrolyte decomposition reaction.

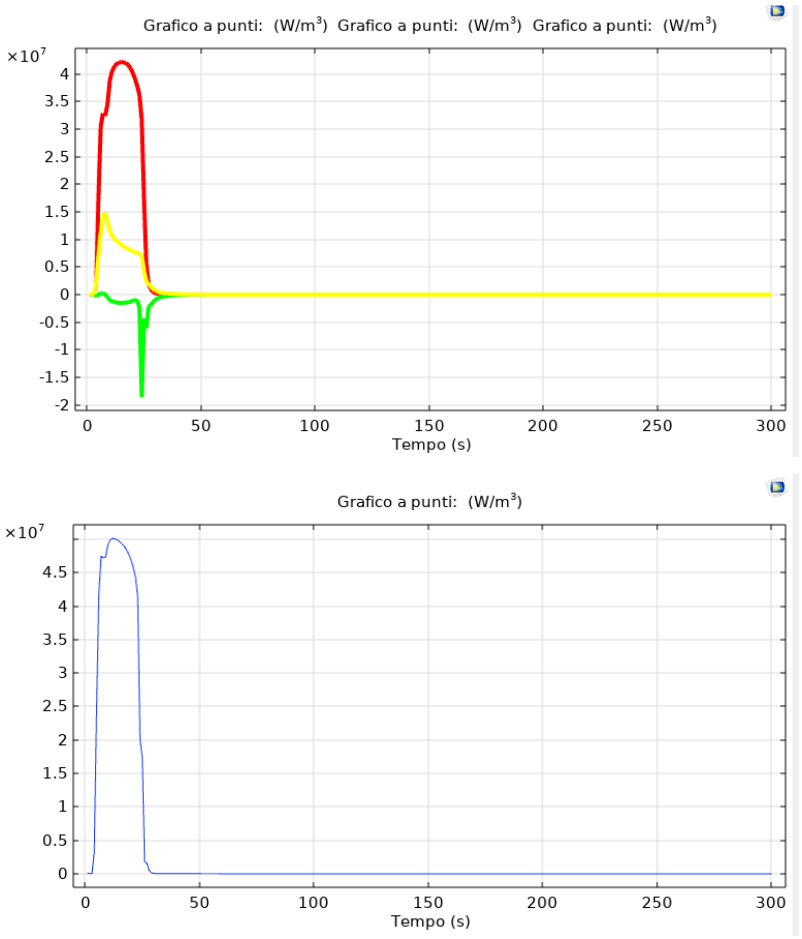

Figure 27 short circuit heat divided by generation source and total short circuit heat

In the proposed modeling framework, the internal short circuit is generated directly within the electrochemical model rather than being imposed as an external boundary condition. This approach allows the short-circuit current to naturally arise from the local electrical and material properties of the cell, making the process inherently driven by the underlying physics of the system. As a result, the magnitude of the short circuit depends on the evolution of variables such as conductivity, potentials, and ionic transport. During the short-circuit phase, the dominant contribution to heat generation is the ohmic term, which is associated with the high current flowing through the internal conductive pathway. This contribution becomes particularly significant due to the reduced resistance between the electrodes, leading to intense Joule

heating. In comparison, the reversible and reaction-related heat terms play a secondary role in this stage, as the system rapidly departs from normal operating conditions and becomes primarily governed by resistive dissipation.

Once the internal short circuit has triggered the initial temperature rise, the subsequent increase in temperature is mainly governed by the activation of the Arrhenius-type reactions included in the model. These reactions are strongly temperature-dependent and introduce a positive feedback mechanism: as the temperature increases, the reaction rates grow exponentially, generating additional heat and further accelerating the process. This leads to a cascade effect, in which different exothermic reactions are sequentially activated as their characteristic onset temperatures are reached. Typically, the first contribution to be activated is associated with the decomposition of the solid electrolyte interphase (SEI), which occurs at relatively low temperatures (≈ 90–120 °C). This is followed by reactions involving the anode and the cathode (≈ 130–200 °C), which further contribute to heat generation. At higher temperatures, usually above 230-280 °C there is the decomposition of the electrolyte releasing a large amount of heat and often representing the most energetic contribution. This ordered activation of reactions reflects the increasing thermal instability runaway, how is illustrated in figure 8 of the work "Characterizing and predicting 21700 NMC lithium-ion battery thermal" [30], induced by nail penetration of the system and sustains the thermal runaway process, even after the initial short-circuit event, ultimately determining the peak temperature reached by the cell.

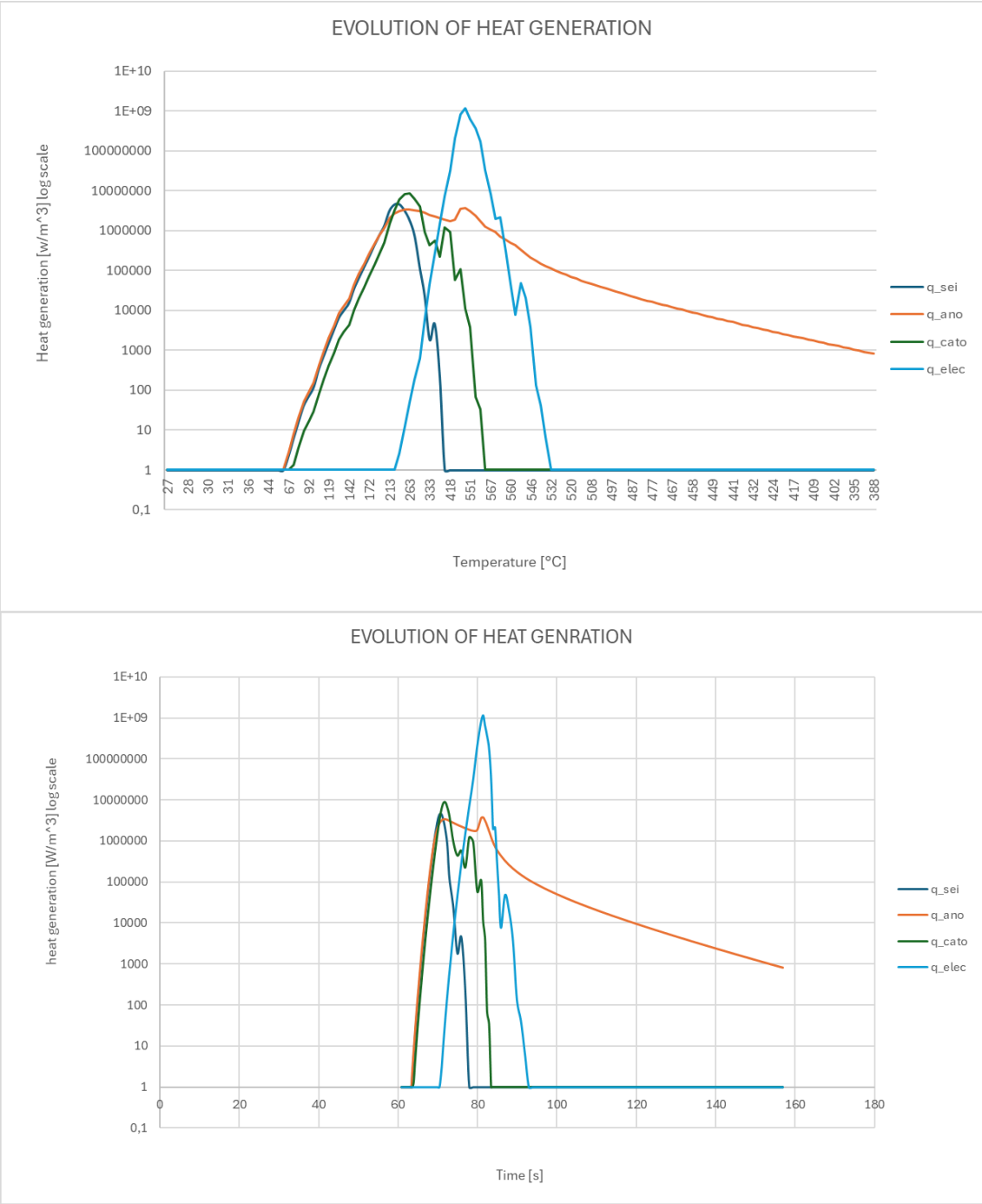

Figure 28 Evolution of heat generation with Temperature and with Time

The evolution of heat generation as a function of temperature highlights the different roles played by each contribution during the thermal runaway process. At relatively low temperatures, the first contribution to become significant is associated with the SEI decomposition (blue curve),

which increases rapidly but remains limited in magnitude compared to the other sources. As the temperature rises, the anode-related heat generation (orange curve) becomes dominant over a wide temperature range, showing a smoother peak and a long tail, indicating that it sustains heat release even at higher temperatures. This behavior can be explained not only by transport limitations, such as lithium diffusion in the solid phase, but also by the kinetic parameters of the Arrhenius law. In particular, a relatively higher activation energy combined with a moderate pre-exponential factor leads to a more gradual increase in the reaction rate with temperature, preventing a sharp and localized peak. As a result, the anode reaction does not rapidly exhaust but instead releases heat over an extended temperature interval. In contrast, the cathode contribution (green curve) activates shortly after the anode, reaching a pronounced peak before rapidly decreasing, suggesting a faster depletion of reactive material. The most intense and localized peak is instead associated with the electrolyte (light blue curve), which exhibits a sharp and high maximum over a narrow temperature interval. This indicates that, once activated, electrolyte decomposition releases a large amount of heat in a short temperature range, significantly contributing to the acceleration of the thermal runaway. Overall, the graph clearly shows a cascade behavior, in which SEI decomposition initiates the process, followed by anode and cathode reactions, and finally by the highly energetic electrolyte decomposition, which dominates the peak heat generation.

	T_start [°C]	Q_max [W/m^3]
SEI	96 °C	4,5 e^6W/m^3
ANODE	96 °C	3.74e^6 W/m^3
CATHODE	110 °C	8.62e^6 W/m^3
ELECTROLYTE	270°C	1.15e^9 W/m^3

Table 5 Critical point of materials decomposition

This table is constructed considering an onset T when the heat generated has a relevant value (=10^2) to give a contribution to the increasing temperature; although the reactions start before the selected time, they have a very slow change and it is not correct consider the runaway has started. It is possible to have a confirmation of this analyzing the graph below that shows that the variation of concentrations starts to have a relevant gradient after reaching higher value of temperature.

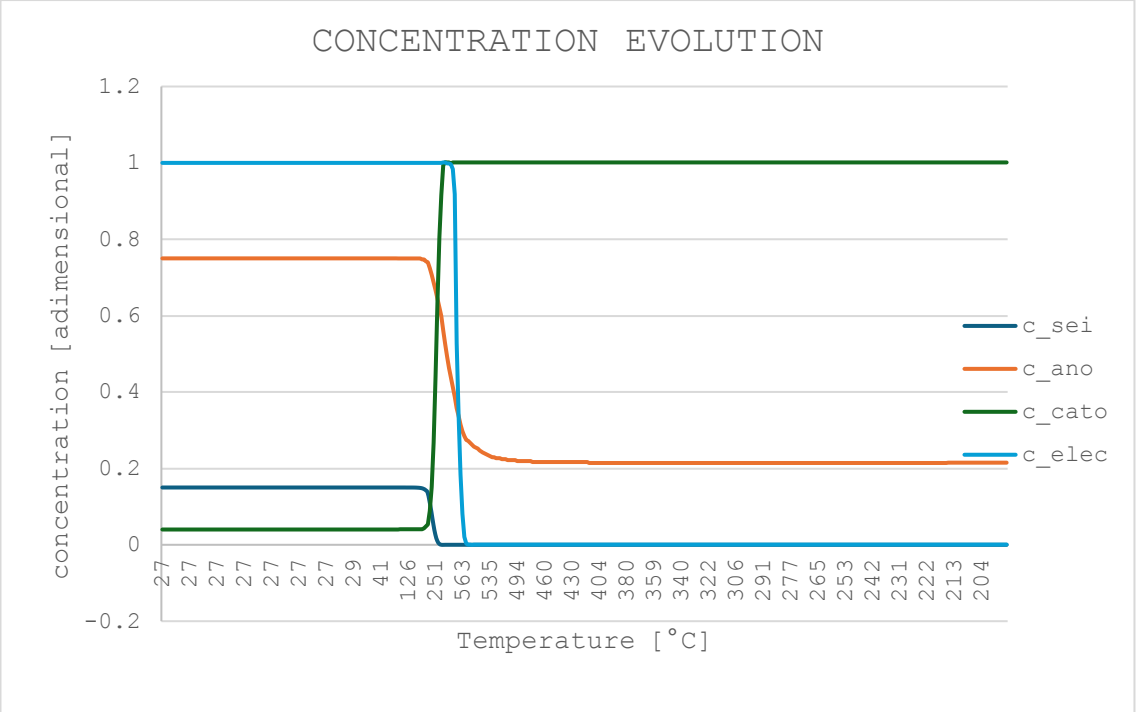

Figure 29 Concentration evolution

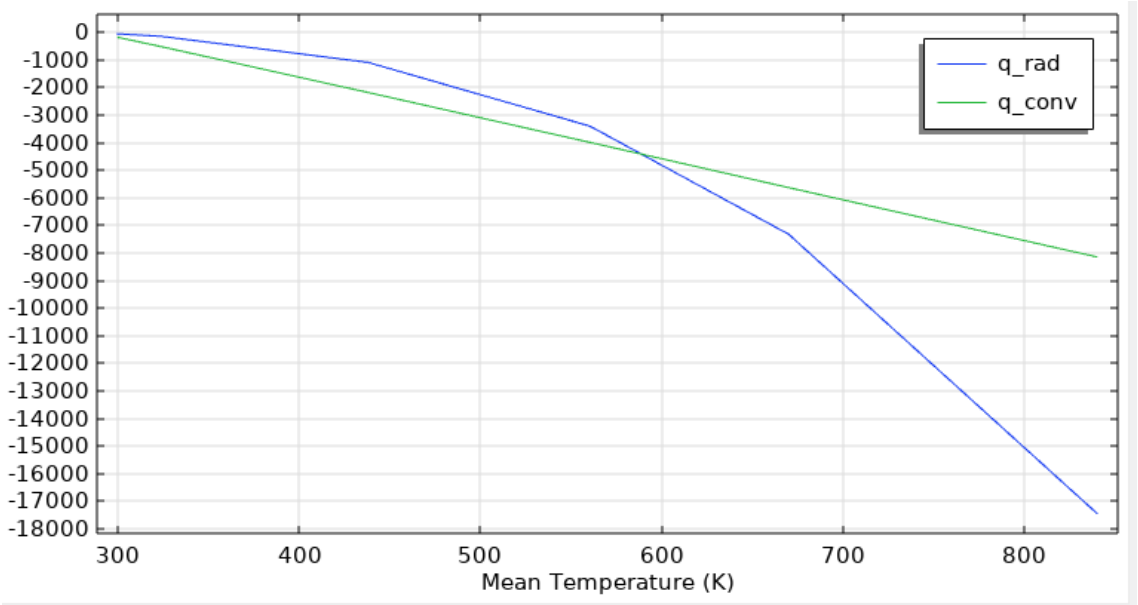

Figure 30 Radiative and Convective heat

The analysis of the dissipative heat contributions highlights the different roles played by convective and radiative heat transfer mechanisms during the thermal evolution of the cell. The convective heat loss follows a linear dependence on temperature difference with respect to the environment. As a result, convection provides a steady and proportional heat dissipation throughout the entire process, but its effectiveness remains limited even at high temperatures. In contrast, radiative heat transfer exhibits a strongly nonlinear behavior, being proportional to the fourth power of temperature according to the Stefan–Boltzmann law. This implies that, while radiation is negligible at low and moderate temperatures, it becomes increasingly significant as the temperature rises. At elevated temperatures, such as those reached during thermal runaway, radiative losses can become comparable to or even exceed convective ones, thus playing a crucial role in limiting the maximum temperature reached by the system. This difference in behavior highlights the importance of including both

mechanisms in the model, especially when simulating high-temperature phenomena.

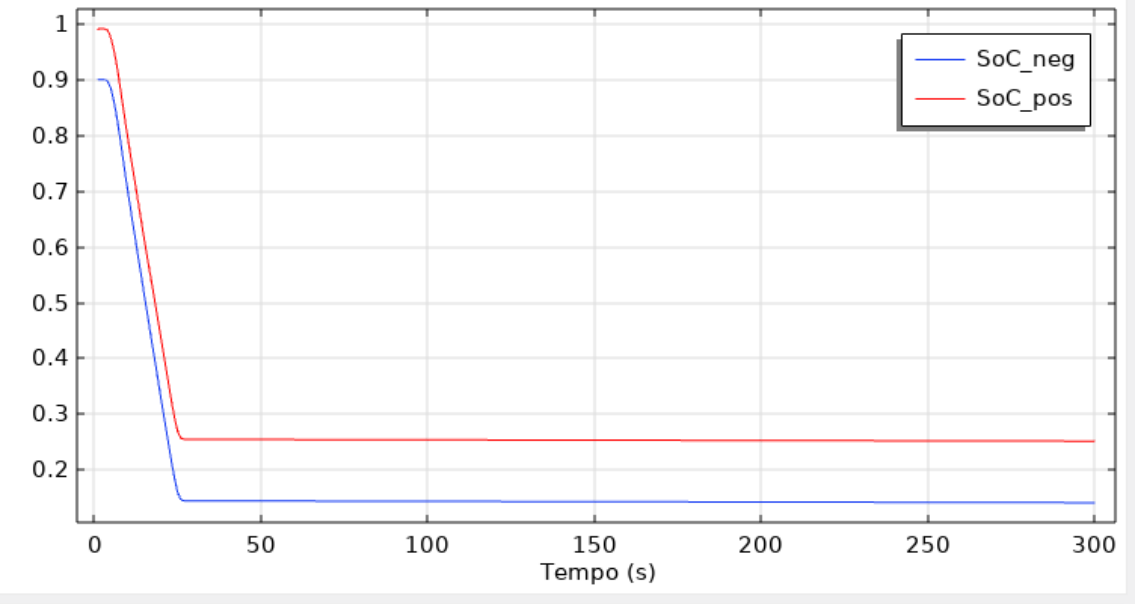

Figure 31 SoC Positive and Negative

The evolution of the state of charge (SOC) during the simulation shows a rapid decrease as a consequence of the internal short-circuit, which forces a high current flow and accelerates the depletion of available lithium. However, the SOC does not reach zero, and instead stabilizes at a residual value. This behavior is not purely physical but is related to the limitations of the electrochemical model under extreme conditions. As the system approaches severe states, transport limitations particularly lithium diffusion in the solid phase and electrolyte become dominant, leading to steep concentration gradients and numerical stiffness. At this point, the solver is no longer able to proceed reliably, and the electrochemical simulation effectively stops evolving. As a result, the remaining SOC reflects the point at which the model ceases to be valid, rather than a complete discharge of the cell. This outcome is consistent with the transition toward a regime where the system behavior is no longer

governed by electrochemical processes, but rather by purely thermal and resistive effects.

6.2 Model–Experiment Comparison

In this chapter, the numerical model developed to simulate the thermal behavior of a lithium-ion cell under high-stress operating conditions is validated. The comparison is performed between the model results (green line) and two independent experimental datasets (red and blue lines).

6.2.1 Analysis of Absolute Temperature Profiles

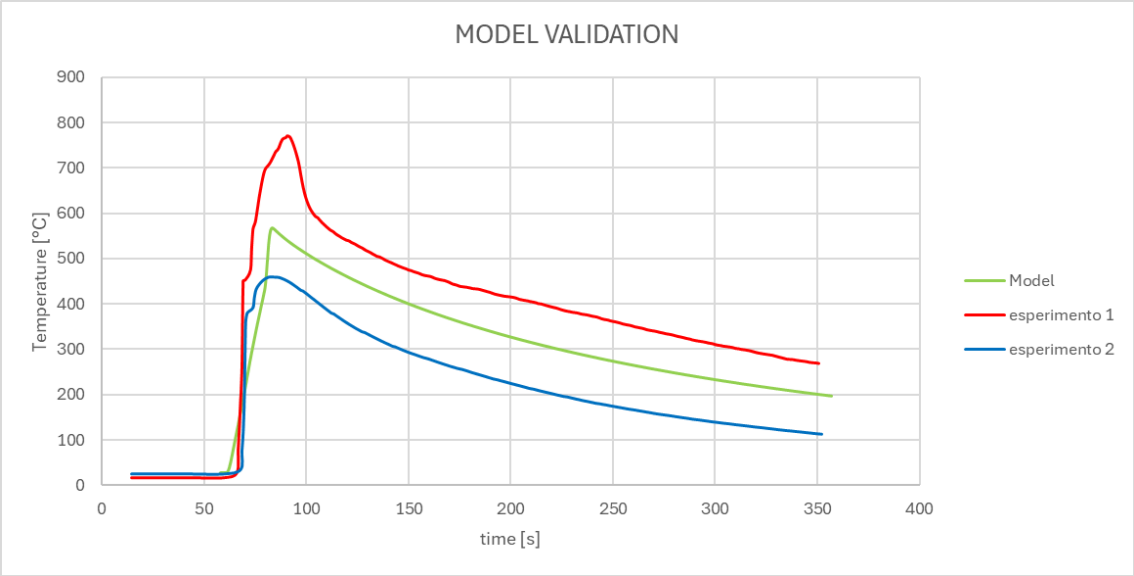

Figure 32 Model-Experiment Comparison

The graph illustrates the evolution of absolute temperature (°C) over time (s). A significant dispersion is observed in the experimental results: Experiment 1 reaches a peak of approximately 780 °C, while Experiment 2 plateaus at 46 °C.

The numerical model (green line) is positioned in an intermediate range, with a peak of approximately 570 °C. This modeling approach represents a robust average behavior, accounting for intrinsic variations such as contact resistances, cell-to-cell manufacturing differences, or fluctuations in ambient conditions during the experimental setup.

6.2.2 Normalized Data Analysis and Temporal Dynamics

To accurately assess the model's temporal fidelity, a normalization was performed as shown in figure 39. Each curve was normalized by dividing it by its own local maximum value, bringing all peaks to a unitary value.

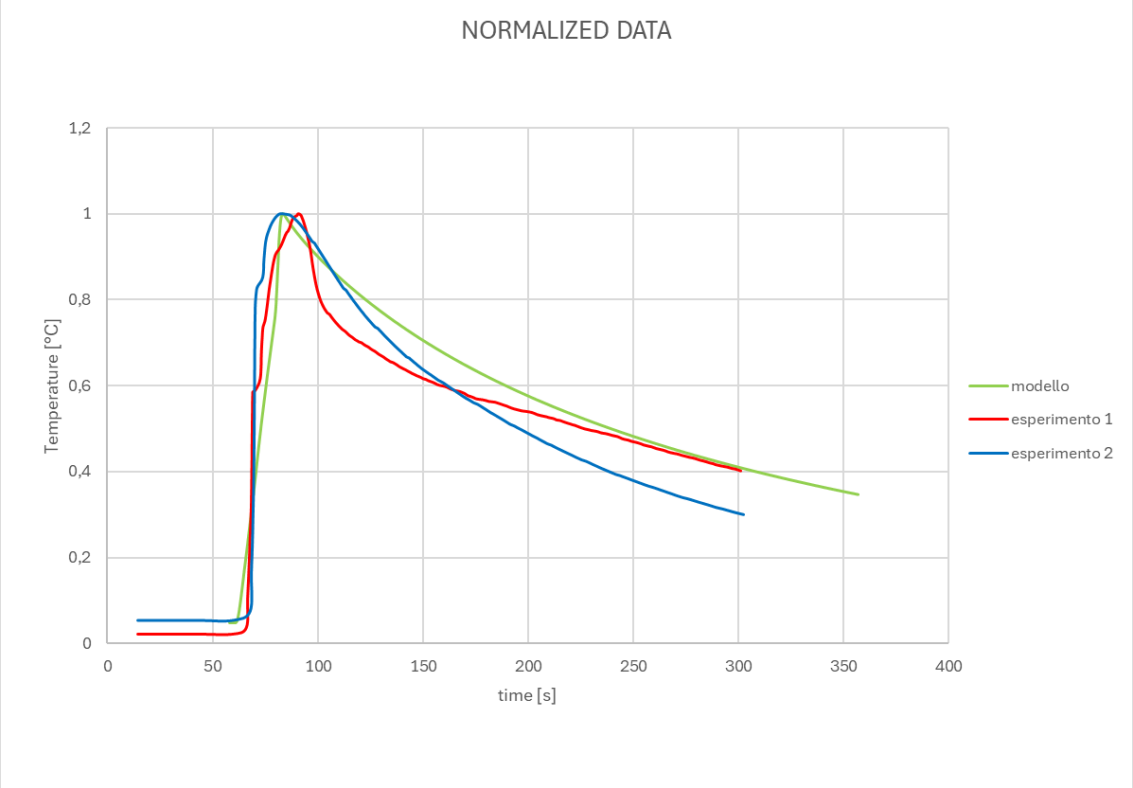

Figure 33 Normalized comparison between model and experiments

The analysis of this graph provides critical insights into the physics of the phenomenon:

- Peak Position and Synchronization: The model (green line) reaches its peak in perfect synchronization with Experiment 2 (blue line), while it anticipates the peak of Experiment 1 (red line). This behavior suggests that the model's thermal inertia is accurately calibrated for the dynamics of the blue curve. The delay observed in Experiment 1

is primarily due to the much higher absolute temperature reached; since Experiment 1 targets a significantly higher energy state, it requires a more extended accumulation phase before reaching its maximum value.

The accuracy of the model was evaluated by calculating the percentage error at the peak value with respect to the average value of the experimental tests. This choice is motivated by the variability observed among the experiments. The resulting percentage error indicates a good capability of the model to predict the order of magnitude of the phenomenon.

	T_peak [°C]	t_peak [s]	%error_t
1° Experiment	770 [°C]	90.6 [s]	/
2° Experiment	459 [°C]	82.2[s]	/
Model	567 [°C]	83.75 [s]	3.1%

Table 6 Values of the Peaks and Error

- Heating Phase: Despite the variations in peak timing, the initial slope of the model's heating curve (green line) is consistent with the experimental trends. This indicates that the internal heat generation comprising Joule heating and chemical reactions has been correctly implemented within the numerical code.
- Thermal Inertia and Response Time: The alignment with Experiment 2 confirms that the model's heat capacity and internal thermal resistance are well-defined. The slight anticipation compared to

Experiment 1 confirms a physically consistent system: higher thermal intensities necessitate longer saturation times, a phenomenon that the model effectively mediates for design purposes.

- Cooling Dynamics: In the post-peak phase, the model demonstrates a thermal dissipation rate that closely follows the experimental decay; the experiment 1 shows a higher dissipation at high T due to the stronger contribution of radiative heat, but then the trend is well approximated by the model. This validates the environmental heat transfer parameters (convection and radiation), confirming the model's ability to accurately predict the duration required for the cell to return to safety thresholds.

6.3 Discussion of Results

The comparison highlights that the model not only captures the qualitative trend of the thermal event but also correctly identifies the temporal criticalities. The synchronization with Experiment 2 and the consistent slope during the heating phase demonstrates that the model is a reliable tool for predicting the thermal response of the battery, providing a balanced and physically sound representation across different stress levels [30].

6.4 Model Accuracy and Limitations

Despite the encouraging results, several aspects can be further improved in future work. The current formulation is based on a one-dimensional

representation of the cell, which inherently assumes a uniform behavior across the electrode area. Extending the model to two- or three-dimensional geometries would allow the investigation of localized phenomena, such as non-uniform current distribution and hotspot formation, which play a crucial role in real failure scenarios. Moreover, a more detailed description of the short-circuit mechanism, including the evolution of the contact resistance and the effects of mechanical deformation, could enhance the physical accuracy of the model.

Additional developments may also include the integration of more advanced degradation and decomposition kinetics, in order to better capture the complex chain of reactions occurring during thermal runaway. Finally, coupling the model with gas generation and pressure evolution could provide a more comprehensive description of the failure process, further improving its predictive capabilities.

7. Conclusions and Future Developments

The results obtained in this work demonstrate that the proposed electrochemical–thermal model is able to capture the main features of the cell behavior under internal short-circuit conditions. In particular, the comparison between numerical simulations and experimental data shows a good agreement in terms of temperature evolution and general system response. Although some discrepancies may be observed in the exact timing or magnitude of specific events, the model successfully reproduces the key trends associated with the onset and progression of thermal runaway. This confirms that the adopted modeling approach, based on a coupled electrochemical and thermal framework, is suitable for

describing the dominant physical phenomena involved in battery failure under abuse conditions.

The validation against experimental results obtained through mechanical abuse tests provides further confidence in the reliability of the model. The ability to reproduce the thermal response of the cell under nail penetration conditions indicates that the implemented representation of the internal short circuit and the associated heat generation mechanisms are consistent with the observed behavior. In particular, the model captures the rapid temperature increase following the short circuit and the subsequent evolution driven by thermal and electrochemical interactions, which are critical aspects in the study of thermal runaway.

From a safety perspective, the developed model represents a valuable tool for analyzing critical operating conditions and identifying potential failure scenarios in lithium-ion batteries. By enabling the investigation of internal short circuits and their thermal consequences, the model can support the design of safer battery systems and contribute to the development of mitigation strategies aimed at preventing or delaying thermal runaway. For instance, the model can be used to assess the influence of material properties, cell design parameters, and operating conditions on the severity of the failure event.

The modeling framework developed can be further extended, with relatively limited modifications, to investigate multi-cell configurations and study thermal propagation phenomena in battery modules. By coupling several cells in series within the same thermal domain, it is possible to simulate the heat transfer between adjacent cells and analyze how a failure event in one cell can trigger thermal runaway in neighboring units. In this context, the model can be used to evaluate the conditions

under which thermal propagation occurs and to identify critical design parameters influencing its severity. Moreover, the framework can be adapted to include additional components, such as protective layers or encapsulation materials. In particular, the introduction of a Phase Change Material (PCM) surrounding the cells represents a promising passive strategy to mitigate thermal runaway. Thanks to its ability to absorb large amounts of heat during phase transition, the PCM can limit temperature rise and delay or prevent the propagation of thermal runaway to adjacent cells. By incorporating such materials into the model, it becomes possible to assess their effectiveness and optimize their properties and configuration, providing a valuable tool for the design of safer battery systems.

In recent years, increasing attention has been devoted to the development of solid-state batteries, which are considered a promising alternative to conventional lithium-ion technologies. By replacing the liquid electrolyte with a solid ionic conductor, these systems offer significant advantages in terms of safety, thanks to the reduced risk of leakage and thermal runaway, and potentially higher energy density. Despite these benefits, solid-state batteries also introduce new challenges related to ion transport and interfacial phenomena.

The governing equations adopted in this work are based on a continuum electrochemical framework that can, in principle, be extended to describe different battery technologies, including solid-state systems. The conservation equations for charge and mass, as well as the thermal model, retain the same general structure and can be directly reused. However, significant modifications are required in the constitutive relations and in the description of transport and interfacial phenomena. In particular, the absence of a liquid electrolyte leads to different ion transport mechanisms,

while the electrode–electrolyte interfaces are characterized by solid–solid contact effects that are not fully captured by standard Butler–Volmer kinetics. Despite these differences, the modeling approach developed in this work provides a flexible foundation that can be adapted to solid-state batteries through appropriate modifications of material properties and reaction kinetics.

Overall, the modeling approach presented in this work constitutes a solid basis for the analysis of lithium-ion battery safety and offers significant potential for future developments. By combining numerical simulations with experimental validation, the model can contribute to a deeper understanding of thermal runaway phenomena and support the development of safer and more reliable energy storage systems.

Nomenclature

a_s-specific area [1/m]

$brug$- Bruggeman coefficient [-]

c_s -concentration of Li inside the solid [mol/m^3]

cs_{max}-maximum concentration of Li in the solid [mol/m^3]

c_e-concentration of Li inside the electrolyte [mol/m^3]

C_p- specific heat [J/(kg*K)]

D_s-diffusion coefficient inside the solid [m^2/s]

D_e-diffusion coefficient in the electro [m^2/s]

F-Faraday number [C/mol]

NMC- Nickel Manganese Cobalt

Q_{rev}-reversible heat [W/m^3]

Q_{rnx}-irreversible heat [W/m^3]

Q_{ohm}-ohmic heat [W/m^3]

Q_{arr}-Arrhenius Heat [W/m^3]

ε is the porosity [-]

r-coordinate of the particle [m]

t_+^0-transport number of lithium ions [-]

U_{eq}-equilibrium potential [V]

φ_s-solid potential [V]

φ_e-electrolyte potential [V]

η-overvoltage [V]

σ-solid conductivity [S/m]

k- ionic conductivity [S/m]

θ -Utilization factor of electrodes [-]

ρ - electrode density [kg/m^3]

References

[1] Gazzetta ufficiale dell'Unione europea, “Gazzetta ufficiale dell'Unione europea”,2015

[2] European Parliament, “International Climate Negotiations”, 2025

[3] European Parliament, “Green Deal europeo: la chiave per un’UE sostenibile e climaticamente neutrale”, 2025

[4] Samsung SDI Co., Ltd., Specification of Product: INR18650-35E (Version 3), Spec. No. INR18650-35E, v1.0, Nov. 2023.

[5] Wang Q., "A review of lithium ion battery failure mechanisms and fire prevention strategies", Progress in Energy and Combustion Science, 2018.

[6] Li H., "Multi-field interpretation of internal short circuit and thermal runaway behavior for lithium-ion batteries under mechanical abuse", Journal of Energy Storage, 2023.

[7] Abbas M. M., "Simulations-based investigation of thermal runaway onset and propagation in a Li-ion battery pack with phase transition interstitial material", Applied Thermal Engineering, 2025.

[8] Hatchard D., MacNeil D., Basu A., Dahn J., "Thermal model of cylindrical lithium-ion cells", Journal of The Electrochemical Society, 2001.

[9] Spotnitz R., Franklin J., "Abuse behavior of high-power lithium-ion cells", Journal of Power Sources, 2003.

[10] Coman P., Darcy E., Veje C., White R., "Modelling Li-ion cell thermal runaway triggered by an internal short circuit device", Journal of Applied Electrochemistry, 2017.

[11] Doyle M., Fuller T. F., Newman J., "Modeling of Galvanostatic Charge and Discharge of the Lithium/Polymer/Insertion Cell", Journal of The Electrochemical Society, 1993.

[12] Ivanovich T. M., "Analysis of numerical models describing the aging of

lithium-ion batteries due to the formation of an interphase layer of solid electrolyte", Batteries, 2023.
[13] Baek S. W. et al., "Measuring Heat Dissipation and Entropic Potential in Battery Cathodes...", ACS Applied Materials & Interfaces, 2023.
[14] Reynier Y., Yazami R., Fultz B., "The entropy and enthalpy of lithium intercalation into graphite", Journal of Power Sources, 2003.
[15] Chen S.-C., Wang Y.-Y., Wan C.-C., "Thermal Analysis of Spirally Wound Lithium Batteries", Journal of The Electrochemical Society, 2006.
[16] Gomadam P. M., White R. E., "Modeling Heat Conduction in Spiral Geometries", International Journal of Heat and Mass Transfer, 2003.
[17] Maleki H. et al., "Thermal Properties of Lithium-Ion Battery and Components", Journal of The Electrochemical Society, 1999.
[18] COMSOL Multiphysics, "Thermal modelling of a cylindrical Lithium-Ion Battery in 2D", Application ID: 14611, 2023.
[19] Jia Y. et al., "Thermal Runaway propagation behaviour within 18,650 lithium-ion battery packs: A modelling study", Journal of Energy Storage, 2020.
[20] Duan X., "A multiphysics understanding of internal short circuit mechanisms in lithium-ion batteries upon mechanical stress abuse", Thesis/Journal of Power Sources, 2022.
[21] Zavalis T. G. et al., "Investigation of Short-Circuit Scenarios in a Lithium-Ion Battery Cell", Journal of The Electrochemical Society, 2012.
[22] Lai X. et al., "Mechanism, modeling, detection, and prevention of the internal short circuit in lithium-ion batteries: Recent advances and perspectives", Energy Storage Materials, 2021.
[23] Richard M. N., Dahn J. R., "Accelerating Rate Calorimetry Study on the Thermal Stability of Lithium Intercalated Graphite in Electrolyte", Journal of The Electrochemical Society, 1999.

[24] Feng X. et al., "Investigating the thermal runaway mechanisms of lithium-ion batteries based on thermal analysis database", Applied Energy, 2019.
[25] Zhao C. et al., "Thermal runaway hazards investigation on 18650 lithium-ion battery using extended volume accelerating rate calorimeter", Journal of Energy Storage, 2020.
[26] Musso L., "Sicurezza delle batterie di veicoli elettrici in condizioni critiche", Tesi di Laurea, Politecnico di Torino, 2024.
[27] Chen Y. et al., "Accurate voltage prediction for lithium and sodium-ion full-cell development", Nature Communications/Journal Citation, 2024.
[28] Yu Q.-Q. et al., "A Comparative Study on Open Circuit Voltage Models for Lithium-ion Batteries", Chinese Journal of Mechanical Engineering, 2018.
[29] Wind J. et al., "Entropy Profiles for Li-Ion Batteries, Effects of Chemistries and Degradation", Journal of The Electrochemical Society, 2025. [30] SAMSUNG SDI, “Safety Data Sheet”, 2020

[30] A. V. Shelke et al., "Characterizing and predicting 21700 NMC lithium-ion battery thermal runaway induced by nail penetration," Applied Thermal Engineering, vol. 209, p. 118278, Jun. 2022

[31] Kim G.-H., Pesaran A., Spotnitz R., "A three-dimensional thermal abuse model for lithium-ion cells", Journal of Power Sources, 2007.

[32] Mallick S., Gayen D., "Thermal behaviour and thermal runaway propagation in lithium-ion battery systems – A critical review", Journal of Energy Storage, 2023.

[33] Tran M.-K., Mevawalla A., Aziz A., Panchal S., Fowler M., Fraser R., "A Review of Lithium-Ion Battery Thermal Runaway Modeling and Diagnosis Approaches", Processes, 2022.